uOttawa

L'Université canadienne
Canada's university

FACULTÉ DES ÉTUDES SUPÉRIEURES ET POSTDOCTORALES

uOttawa

L'Université canadienne
Canada's university

FACULTY OF GRADUATE AND POSTDOCTORAL STUDIES

Alura Elizabeth Riley

AUTEUR DE LA THÈSE / AUTHOR OF THESIS

M.Sc. (Biochemistry)

GRADE / DEGREE

School of Translation and Interpetation

FACULTÉ, ÉCOLE, DÉPARTEMENT / FACULTY, SCHOOL, DEPARTMENT

Regulation of the X-linked Inhibitor of Apoptosis Protein (XIAP) Expression through Alternative Non-Coding Regions

TITRE DE LA THÈSE / TITLE OF THESIS

M. Holcik

DIRECTEUR (DIRECTRICE) DE LA THÈSE / THESIS SUPERVISOR

CO-DIRECTEUR (CO-DIRECTRICE) DE LA THÈSE / THESIS CO-SUPERVISOR

EXAMINATEURS (EXAMINATRICES) DE LA THÈSE / THESIS EXAMINERS

J. Côté

M. Pelchat

Gary W. Slater

Le Doyen de la Faculté des études supérieures et postdoctorales / Dean of the Faculty of Graduate and Postdoctoral Studies

REGULATION OF THE X-LINKED INHIBITOR OF APOPTOSIS PROTEIN (XIAP) EXPRESSION THROUGH ALTERNATIVE NON-CODING REGIONS

By

Alura Riley

Thesis submitted to the School of Graduate and Post-doctoral studies, University of Ottawa, in partial fulfilment of the requirements for the degree of Master of Science

Department of Biochemistry, Microbiology and Immunology, Faculty of Medicine, University of Ottawa

Your file Votre référence
ISBN: 978-0-494-58201-5
Our file Notre référence
ISBN: 978-0-494-58201-5

Abstract

The X-linked Inhibitor of Apoptosis Protein (XIAP) counters diverse apoptotic pathways through inhibition of caspases. The levels of XIAP protein can be increased translationally in response to pathophysiological stress, elevating the apoptotic threshold of cells. Here, I have characterized two XIAP mRNA isoforms, which differ only in their 5' untranslated regions. When global translation is attenuated during pathophysiological stress, the translation of one XIAP mRNA isoform is dramatically increased through the action of an Internal Ribosome Entry Site (IRES). In contrast, the second XIAP mRNA isoform supports cap-dependent translation of XIAP, but does not contain a functional IRES element. The physiological relevance and contribution of the XIAP mRNA variants to XIAP protein levels have been examined using RNA Interference, in conjunction with a cellular stress model. The distinct translational activities of these two transcripts under cellular stress suggest a model for a dual mode of XIAP regulation, which may be a common mechanism.

Acknowledgements

I would like to express my gratitude to my supervisor, Dr. Martin Holcik, for his commitment to his work and his students, and of course, for his unrelenting optimism. One could not ask for a more involved, knowledgeable and supportive supervisor. I would also like to thank my Thesis Advisory Committee members Dr. Jocelyn Côté and Dr. David Stojdl, for helpful discussions and direction. Many thanks to the Holcik lab for making the time spent on this research seem too much fun to be work. Thanks also to all members of the Apoptosis Research Centre, as well as to the Children's Hospital of Eastern Ontario and the University of Ottawa. I would also like to acknowledge the Canadian Institutes of Health Research and the Government of Ontario for provision of funding that enabled this work.

I dedicate this thesis, and the immense amount of work that went into it, to my mother Anne Riley. You are an amazing example of how much one person is capable of in a lifetime, and you are and always have been a great inspiration to me.

Table of Contents

List of Abbreviations

ATP – adenosine triphosphate

Bag-1 – Bcl2-associated athanogene

BIR – baculoviral IAP repeat

βgal – beta-galactosidase

BSA – bovine serum albumin

CAT – chloramphenicol acetyltransferase

cDNA – complementary deoxyribonucleic acid

CHX - cycloheximide

CIAP – cellular inhibitor of apoptosis

ct – cycle threshold

DMEM – Dulbecco's modified Eagle medium

DNA – deoxyribonucleic acid

EDTA – ethylenediaminetetraacetic acid

eIF – eukaryotic initiation factor

ELISA – enzyme-linked immunosorbent assay

ER – endoplasmic reticulum

EtBr – ethidium bromide

EST – expressed sequence tag

Fas – Apoptosis stimulating fragment

FGF-1 – fibroblast growth factor 1

FBS – Fetal bovine serum

GAPDH - glyceraldehyde-3-phosphate dehydrogenase

GDP – guanosine diphosphate

GTP – guanosine triphosphate

HEK293 – human embryonic kidney 293 cells

hnRNP – heterogenous nuclear ribonucleoprotein

HP - hairpin

HPV – human papilloma virus

HRP – horseradish peroxidase

IAP – inhibitor of apoptosis

IRES – internal ribosome entry site

ITAF – IRES *trans*-acting factor

IVT – *in vitro* transcription

kb - kilobase

KGM – keratinocyte growth medium

L-UTR – long untranslated region (of XIAP)

m7G – 7-methylguanosine (cap)

mRNA – messenger ribonucleic acid

mTOR – mammalian target of rapamycin

NAIP – neuronal apoptosis inhibitory protein

NEO – neomycin phosphotransferase II

Omi/HtrA2 – Omi/high temperature requirement A2

nt - nucleotide

PABP – poly(A) binding protein

PBS – phosphate-buffered saline

PCBP1 – poly(rC) binding protein 1

PCR – polymerase chain reaction

PMSF – phenylmethylsulfonyl fluoride

PPT – polypyrimidine tract

PTB – polypyrimidine tract binding protein

qRT-PCR – quantitative real-time polymerase chain reaction

RING – really interesting new gene

RIPA - radioimmunoprecipitation assay

RNA – ribonucleic acid

RNAi – RNA interference

rpS6 – ribosomal protein S6

RT – reverse transcription

S-UTR – short untranslated region (of XIAP)

SDS-PAGE – sodium dodecyl sulfate-polyacrylamide gel electrophoresis

siRNA – small interfering RNA

Smac/Diablo – second mitochondria-derived activator of caspases/direct inhibitor of apoptosis-binding protein with a low isoelectric point

TAB1 – TGF-β-activated protein kinase 1- binding protein 1

TGF-β – transforming growth factor beta

TOP – terminal oligopyrimidine tract

TRAIL – tumour necrosis factor–related apoptosis-inducing ligand

tRNA – transfer ribonucleic acid

unr – upstream of N-ras

UTR – untranslated region

X-DC – X-linked dyskeratosis congenita

XIAP – X-linked inhibitor of apoptosis

XLP – X-linked lymphoproliferative syndrome

List of Figures

Chapter 1: Introduction

1.1 Programmed Cell Death

When a cell is no longer deemed beneficial to the functioning of an organism, a controlled cell death program is activated. This process, termed apoptosis, differs from necrotic cell death in that it is a programmed and monitored cell death, requiring energy for execution. It is microscopically characterized by nuclear fragmentation, chromatin condensation and the presence of membrane irregularities, such as apoptotic blebs. To contrast, necrosis occurs when cellular energy is completely depleted, and the cell essentially falls apart (reviewed in Wyllie, 1981). There are also variations of cell death (autophagy, anoikis) that cannot be clearly defined as apoptosis or necrosis. Apoptosis encompasses a number of steps, all converging on the same effector molecules: the caspases. The caspases are a family of cysteine proteases, which bring about cell death through cleavage of key cellular proteins (Cryns, and Yuan, 1998; Thornberry, and Lazebnik, 1998). In normal cell growth conditions, caspases are present in the cell as inactive caspase zymogens. Importantly, caspases are arranged into a cascade, such that activation and proteolytic cleavage of the initiator caspases, such as caspase-9, results in subsequent activation of downstream, or effector, caspases such as caspase-3 (reviewed in Kumar, 2007).

Initiation of a caspase cascade can occur through three distinct pathways: intrinsic, extrinsic, and the endoplasmic reticulum-mediated pathway (outlined in Figure 1). Upon detection of intracellular stress, such as DNA damage, cytochrome *c* is released from the mitochondrial membrane. This activates the intrinsic apoptotic pathway which, following the formation of the apoptosome, results in the activation of caspase-9, an initiator caspase (Acehan, Jiang, et al, 2002; Li, Nijhawan, et al, 1997). The endoplasmic

Figure 1: Apoptosis in Mammalian Cells
The apoptotic cascade is complex and there are various layers of regulation imposed on it. There are numerous apoptotic triggers and effectors, as well as many distinct inhibitors. The extrinsic pathway is generally triggered by receptor binding while the intrinsic pathway revolves around the cellular organelles, more specifically the mitochondria and endoplasmic reticulum. Stimulation of either of these pathways results in the activation of caspases, proteins that carry out the destructive work of disassembling the cell. When a cell is stimulated to begin the process of apoptosis, there are a few ways that the cascade can be halted, allowing the cell to recover from the apoptotic signal. The inhibitor of apoptosis proteins play critical roles in this response. The most potent of these, the X-linked inhibitor of apoptosis (XIAP), can bind and inhibit both initiator and effector caspases with high efficiency. Since all apoptotic pathways converge on the same caspase effector molecules, XIAP can delay or even inhibit apoptosis initiated from many different stimuli. Figure from (Holcik, and Sonenberg, 2005).

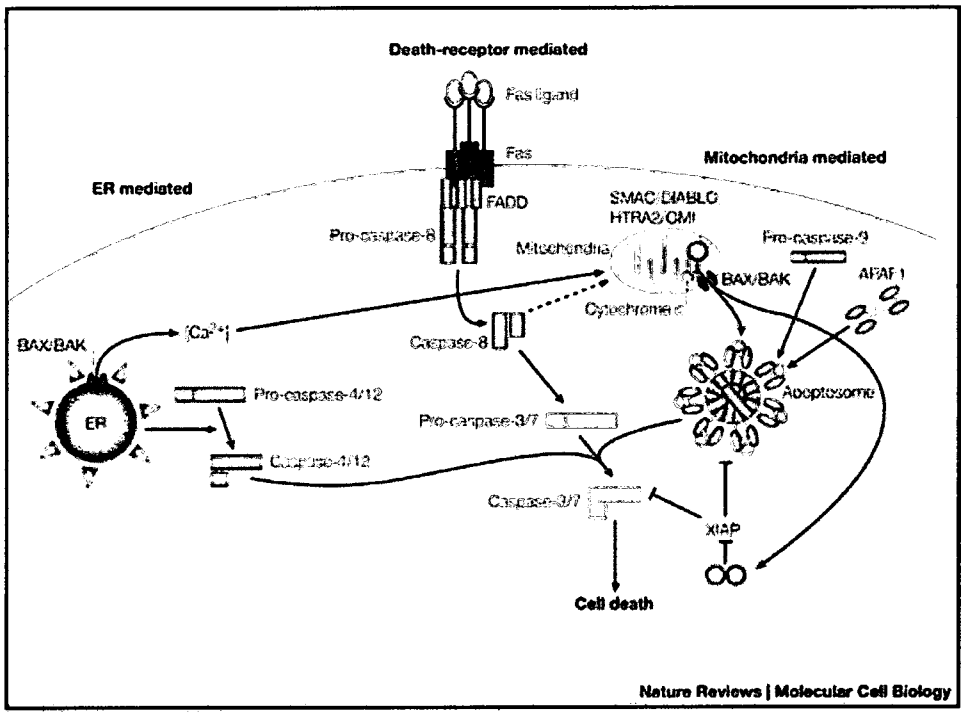
Death-receptor mediated
Fas ligand
Fas
FADD
Pro-caspase-8
ER mediated
Mitochondria mediated
SMAC/DIABLO
HTRA2/OMI
Mitochondria
Pro-caspase-9
BAX/BAK
APAF-1
Cytochrome c
BAX/BAK
[Ca2+]
Caspase-8
ER
Pro-caspase-4/12
Caspase-4/12
Pro-caspase-3/7
Apoptosome
Caspase-3/7
XIAP
Cell death
Nature Reviews | Molecular Cell Biology

reticulum (ER) has more recently been described as an additional site for the initiation of apoptosis, where the accumulation of unfolded proteins results in the activation of ER stress-specific initiator caspases (caspase-2 and -4) (Kuwana, and Newmeyer, 2003; Morishima, Nakanishi, et al, 2002; Oyadomari, and Mori, 2004; Rao, Ellerby, and Bredesen, 2004). Signals from the external cellular environment can also initiate activation of apoptotic death, through activation of the death-receptor mediated pathway. This pathway is initiated upon binding of a specific ligand (such as FasL) to its cognate cell surface receptor (such as Fas) and results in activation of caspase-8 (Boldin, Goncharov, et al, 1996). Irrespective of how the apoptosis was triggered, all of these apoptotic pathways converge in activation of the effector caspases, such as caspase-3 and caspase-7 (Degterev, Boyce, and Yuan, 2003; Fuentes-Prior, and Salvesen, 2004; Porter, and Janicke, 1999). These proteases are responsible for the progressive disassembly of the cell.

Since inappropriate activation of apoptosis would have devastating consequences, many layers of strict regulation are imposed on the apoptotic pathways. Anti-apoptotic members of the Bcl-2 family are critical to maintaining mitochondrial outer membrane integrity (Gross, McDonnell, and Korsmeyer, 1999; Kuwana, and Newmeyer, 2003; Vander Heiden, and Thompson, 1999). Their actions are crucial to barring the release of pro-apoptotic factors, including cytochrome *c*, into the cytoplasm. This regulation is important to delay or prevent mitochondrial-driven apoptosis, but has less of a role in the other pathways. Alternative control of apoptotic pathways is executed via the Inhibitors of Apoptosis proteins, or IAPs, that are direct caspase inhibitors (Deveraux, Takahashi, et al, 1997; Deveraux, and Reed, 1999).

1.2 The Inhibitor of Apoptosis Proteins

The Inhibitors of Apoptosis were initially discovered in baculovirus, but subsequent studies have found homologues in many viruses and eukaryotes (Crook, Clem, and Miller, 1993; Uren, Coulson, and Vaux, 1998). The discovery of a similar protein in humans, the neuronal apoptosis inhibitor protein (NAIP), led to the identification of at least eight human IAPs (Deveraux, and Reed, 1999; Liston, Roy, et al, 1996; Miller, 1999). The functions of these homologous proteins have diverged, with some IAPs retaining the ability to inhibit caspases, and others functioning as ubiquitylases and/or signalling molecules (Eckelman, and Salvesen, 2006; Li, Yang, and Ashwell, 2002; Samuel, Welsh, et al, 2006; Tenev, Zachariou, et al, 2005; Varfolomeev, Wayson, et al, 2006). A common domain found in all IAPs is the baculoviral IAP repeat (BIR). The BIR domains and their associated linker regions are critical for caspase inhibition, although this is not the function of all BIR domains (Deveraux, and Reed, 1999; Miller, 1999; Salvesen, and Duckett, 2002; Shi, 2002; Verhagen, Coulson, and Vaux, 2001). In terms of apoptotic inhibition, the most potent member of the IAP family is the X-linked inhibitor of apoptosis (XIAP). Although the field is conflicted, it is becoming more accepted that although other IAPs may inhibit apoptosis, XIAP is the only one to do so through direct caspase inhibition (Eckelman, and Salvesen, 2006). In specific situations, such as Apo2L/TRAIL-induced apoptosis, the presence of XIAP at sufficient levels is the single most important determinant of cellular survival (Chawla-Sarkar, Bae, et al, 2004). XIAP is critical to the regulation of apoptosis, as it can directly bind and inhibit caspases-3, -7 and -9, with very high affinity (Chai, Shiozaki, et al, 2001; Huang, Park, et al, 2001; Riedl, Renatus, et al, 2001; Scott, Denault, et al, 2005; Shiozaki, Chai, et al, 2003; Srinivasula, Hegde, et al, 2001; Sun, Cai, et al, 2000). XIAP is also capable of binding procaspase-9 and preventing its activation, allowing XIAP to keep the initiator

caspases in check even in the absence of apoptotic stimulus (Deveraux, Roy, et al, 1998). The three distinct BIR domains of XIAP allow the inhibition of distinct caspases (Shi, 2002). The BIR2 domain and its associated linker region are critical for the inhibition of caspase-3 and -7, while the BIR3 domain is necessary for inhibition of caspase-9 (Chai, Shiozaki, et al, 2001; Huang, Park, et al, 2001; Riedl, Renatus, et al, 2001; Scott, Denault, et al, 2005; Shiozaki, Chai, et al, 2003; Srinivasula, Hegde, et al, 2001; Sun, Cai, et al, 2000). The BIR1 domain has also recently been shown to play a role in the TGF-β-activating kinase complex, by specifically binding to an upstream component, TAB1 (Lu, Lin, et al, 2007).

Recent research has identified a critical regulatory role for the RING (really interesting new gene 1) domain of XIAP (Huang, Joazeiro, et al, 2000; Varfolomeev, Blankenship, et al, 2007; Vaux, and Silke, 2005; Vince, Wong, et al, 2007; Yang, Fang, et al, 2000). As well as being necessary for dimerization, this domain acts as an ubiquitin E3 ligase, which can target numerous substrates for destruction, including different caspases and XIAP itself (Silke, Kratina, et al, 2005).

The inhibition of apoptosis by the IAPs can be relieved through the actions of proapoptotic factors, such as Smac/Diablo and Omi/HtrA2, which can inhibit the IAPs (Du, Fang, et al, 2000; Hegde, Srinivasula, et al, 2002; Martins, Iaccarino, et al, 2002; Suzuki, Imai, et al, 2001; van Loo, van Gurp, et al, 2002; Verhagen, Ekert, et al, 2000; Verhagen, Silke, et al, 2002).

Since the above interactions are mainly reversible, the balance between apoptosis and survival rests on the relative concentrations of pro- and anti-apoptotic factors, which is why several mechanisms exist in the cell to maintain this balance. Upon receipt of apoptotic stimuli, one of the first responses in the cell is to inhibit global protein translation, likely to conserve cellular energy and prevent synthesis of non-essential or

potentially detrimental proteins (Mathews, Sonenberg, and Hershey, 2000; Rudra, and Warner, 2004; Warner, 1999). However, since XIAP protein is required to protect the cell from apoptosis, XIAP has evolved a mechanism to evade this translational block. The 5' untranslated region (UTR) of the XIAP transcript contains an internal ribosome entry site, or IRES (Holcik, Lefebvre, et al, 1999). This element allows XIAP protein production to be maintained even when the global protein synthesis machinery has been compromised.

1.3 IRES and Translation

IRES elements were first discovered in picornaviruses, but they were subsequently found in many viruses and eukaryotes (Hellen, and Sarnow, 2001; Jang, Krausslich, et al, 1988; Pelletier, and Sonenberg, 1988). According to the IRESite database, over 60 viral IRESes and close to 100 cellular IRESes have been identified and tested (Mokrejs, Vopalensky, et al, 2006). It has been noted that significant mechanistic differences exist between cellular and viral IRESes, although it is believed that all of these elements are capable of direct ribosome recruitment, and do not require interaction with the mRNA cap or the cap-binding protein (eIF4E).

To understand the relevance of IRES-mediated translation initiation, "normal" or cap-dependent translation initiation will be first reviewed (see Figure 2 for an overview of the differences between these modes of translation). Protein synthesis is a complex process that can be divided into three stages: initiation, elongation and termination. The rate-limiting step – requiring over 25 proteins – is translation initiation, when the ribosome binds an mRNA and begins to synthesize its encoded protein (reviewed in Gebauer, and Hentze, 2004; Hershey, and Merrick, 2000; Johnstone, and Lasko, 2001; Pestova, Kolupaeva, et al, 2001). The first step in this process is the formation of the ternary

Figure 2: The mechanisms of eukaryotic translation initiation.
Initiation of protein translation in eukaryotes is a complex process requiring many factors. Most translation initiation in the cell proceeds through a mode dependent on the binding of the ribosome to the 7-methylguanosine cap of the RNA, and scanning to the first start codon in the correct context. This translational mode, known as cap-dependent translation, is initiated through binding of the eukaryotic initiation factor 4E (eIF4E) to the m7G cap of the mRNA. eIF4E, also known as the cap-binding protein binds eIF4G, a scaffolding protein, which in turn binds eIF3. Since eIF3 is associated with the 40S subunit of the ribosome, the ribosome is recruited to the mRNA, and scanning toward the start codon begins, assisted by the helicase activity of eIF4A, which is also associated with eIF4G. The 40S ribosomal subunit also binds eIF2, which associates with the initiator Met-tRNA. Once the Met-tRNA anticodon recognizes the appropriate start codon, the 60S subunit is recruited and translation begins. Many initiation factors are necessary for this mode of translation, and the presence and integrity of both the cap and the cap-binding protein are critical.
Translation initiation mediated through an internal ribosome entry site (IRES) does not require the cap-binding protein, or even the m7G cap. This mode of translation initiation requires the actions of IRES-*trans* acting factors or ITAFs, the subset of which appears to be specific for each IRES. Identified ITAFs include PTB, hnRNPA1, La and unr. Some IRESes do not require ITAFs or initiation factors, although which factors are necessary seems to be IRES-specific. In IRES-mediated translation the ribosome is recruited directly to, or quite near to, the start codon. Figured modified from (Lopez-Lastra, Rivas, and Barria, 2005).

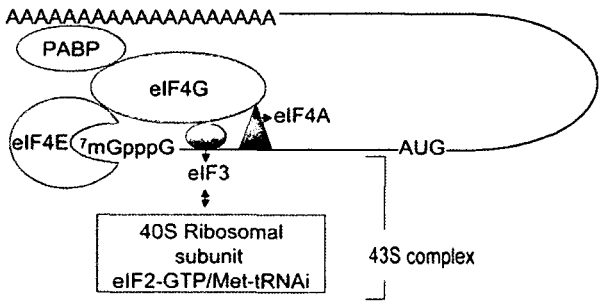

Cap-dependent translation initiation

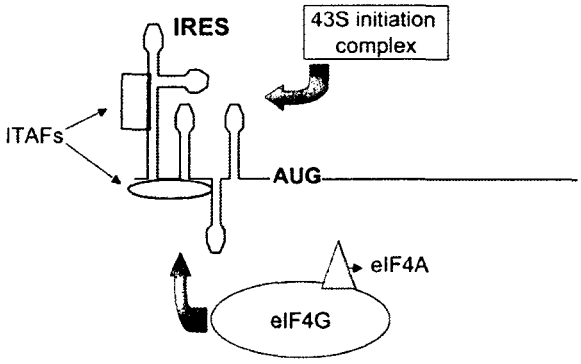

Cap-independent (IRES) translation initiation

complex. This complex consists of GTP-bound eukaryotic initiation factor 2 (eIF2), and the methionine-bound initiator tRNA. The ternary complex associates with the 40S ribosomal subunit to form the 43S pre-initiation complex. The pre-initiation complex also contains other eIFs: eIF1, 1A, 3 and 5. eIF3, and subsequently the pre-initiation complex, is recruited to a transcript through its interaction with the eIF4F complex. eIF4F consists of eIF4E (the cap-binding protein), eIF4A (a DEAD-box RNA helicase) and eIF4G (a large scaffolding protein) (reviewed in Gebauer, and Hentze, 2004). Since eIF4E binds the 7-methylguanosine cap of the mRNA, eIF4F and the associated 43S pre-initiation complex are therefore recruited to the 5' end of the transcript (Marcotrigiano, Gingras, et al, 1997). Once the pre-initiation complex has been recruited to the transcript, eIF4A, with the help of eIF4B, is believed to unwind secondary structure in the 5'UTR of the transcript, enabling the ribosome to scan until it reaches the first AUG start codon in the correct context (Kozak, 1983; Kozak, 1986; Kozak, 1987a; Kozak, 1987b). This process consumes ATP, and is assisted by eIF1, eIF1A and eIF4F (Pestova, Borukhov, and Hellen, 1998; Pestova, and Kolupaeva, 2002). Once the correct start codon is recognized and bound, forming the 48S initiation complex, the eIF2-associated GTP is hydrolysed by eIF5; most of the initiation factors are subsequently released. The 60S ribosomal subunit is then recruited and the process of elongation begins. The process outlined above is used by the majority of cellular mRNAs, although, as mentioned previously, alternative mechanisms exist. In the early 1980s, it was observed that the viral RNA produced during picornaviral infection lacked the 7-methylguanosine cap, yet was still efficiently translated by the host cell machinery (Wimmer, 1982). Subsequent work to elucidate this mechanism found that picornaviral RNAs made use of an internal ribosome entry site (or IRES) to directly recruit the ribosome to the vicinity of the start codon (Jang, Krausslich, et al, 1988; Pelletier, and Sonenberg, 1988). IRESes are

elements found in the 5'UTR of mRNA transcripts, which allow ribosomal recruitment that is independent of binding to the mRNA cap.

Under cellular stress conditions like serum deprivation or viral infection, the cell needs to translate subsets of proteins in order to react to the stress. This necessary translation reprogramming is often initiated through the actions of an IRES, although this is not always the case. Alternate methods of translation that can continue under some types of stress include ribosome shunting and leaky scanning (Futterer, Kiss-Laszlo, and Hohn, 1993; Hinnebusch, 1997; Kozak, 1989b; Morris, and Geballe, 2000; Yueh, and Schneider, 1996; Yueh, and Schneider, 2000).

Many identified viral IRESes share some sequence and/or structure, but the same does not hold true for cellular IRESes (Baird, Turcotte, et al, 2006). It has also been noted that many viral IRESes require little or no protein factors to initiate translation (reviewed in Hellen, and Sarnow, 2001). Cellular IRESes, while bypassing the need for eIF4E, have differing requirements for the other canonical initiation factors (Spriggs, Cobbold, et al, 2009). They also require a host of accessory proteins to initiate translation. These proteins are collectively known as IRES *trans*-acting factors or ITAFs (reviewed in Spriggs, Bushell, et al, 2005). Some ITAFs appear to be required for general IRES translation, while others seem to be specific to a subset of IRESes. For example, the polypyrimidine-tract-binding protein (PTB) has been found to increase translation of many cellular IRESes, although its role can also be inhibitory (Cornelis, Tinton, et al, 2005; Mitchell, Spriggs, et al, 2005; Pickering, Mitchell, et al, 2004). It is unclear how ITAFs modulate IRES function, but it has been proposed that they may participate in RNA remodelling and recruitment of other factors (reviewed in Spriggs, Bushell, et al, 2005). An IRES/ITAF interaction that has been well characterized is that of the Bag-1 IRES with its ITAFs PTB and poly(rC) binding protein 1 (PCBP1). These ITAFs have

been demonstrated *in vitro* and *in vivo* to work in a co-ordinated manner to allow IRES-mediated translation (Pickering, Mitchell, et al, 2003). The primary function of PCBP1 appears to be opening the IRES structure to allow PTB-1 to bind. PTB-1 can then participate in ribosomal recruitment (Pickering, Mitchell, et al, 2004).

Although IRESes vary substantially in terms of their structures, sequences and ITAF requirements, they all share one important feature: the capacity to initiate translation without the involvement of the mRNA cap. This ability becomes important under conditions of cellular stress, when the translation machinery is often modified to attenuate global protein synthesis.

1.4 Regulation of Translation in Stress

Translation initiation is the rate-limiting step in protein synthesis, and hence a common regulatory target. One way in which it is regulated is the inhibition of recycling of the ternary complex, through phosphorylation of Serine-51 on eIF2's α subunit (reviewed in Gebauer, and Hentze, 2004). In normal cell growth, each round of translation initiation hydrolyzes the GTP bound to eIF2 (Hinnebusch, 2000). Phosphorylation of eIF2α increases its affinity for its nucleotide exchange factor eIF2B, trapping it in the inactive eIF2-GDP complex (Abbott, and Proud, 2004). This restricts eIF2B's ability to replenish the cellular pool of eIF2-GTP and protein synthesis is inhibited (Abbott, and Proud, 2004; Clemens, 1994; Hershey, 1991; Hershey, and Merrick, 2000; Proud, 2005; Sonenberg, and Dever, 2003). eIF2 can be phosphorylated in response to various stress conditions (reviewed in Kaufman, 2004; Price, and Proud, 1990; Sonenberg, and Dever, 2003). This modification of the translational machinery strongly inhibits general translation, while increasing translation of specific transcripts (Dever, Feng, et al, 1992).

Another event that occurs in stress situations to regulate global protein synthesis is the sequestration of eIF4E. The initiation factor 4E is critical to the recruitment of the translational apparatus to most mRNAs, as it physically binds the 7-methylguanosine cap with one domain, and interacts with the scaffolding protein eIF4G with another. eIF4E activity is regulated by a family of proteins known as the eIF4E-binding proteins, or 4E-BPs. These proteins compete for the eIF4G-binding site on eIF4E. Under normal growth conditions, the 4E-BPs are hyperphosphorylated, which causes them to have a very low affinity for eIF4E. This allows eIF4E to participate in the eIF4F complex and foster cap-dependent translation initiation. During cellular stress, 4E-BPs are dephosphorylated, greatly increasing their affinity for eIF4E. By binding eIF4E, the 4E-BPs displace eIF4G, disassembling the eIF4F complex (Gingras, Svitkin, et al, 1996). This strongly represses all translation that is dependent on ribosomal recruitment by the mRNA cap (reviewed in Morley, Coldwell, and Clemens, 2005). A related form of translation regulation is the dephosphorylation of eIF4E itself, which has the effect of repressing cap-dependent translation, while stimulating IRES-driven translation (Dyer, Michel, et al, 2003; Pyronnet, Dostie, and Sonenberg, 2001).

A more permanent method of translational repression that can occur in apoptotic and virally infected cells is the specific cleavage of initiation factors. eIF4G, the large scaffolding protein that mediates ribosome recruitment to the mRNA cap, has been demonstrated to undergo cleavage under stress. During picornaviral infection, viral proteases cleave eIF4G in such a fashion as to disconnect its cap-recruiting domain from its ribosome and helicase recruitment domain (reviewed in Prevot, Darlix, and Ohlmann, 2003). The effect of this is that uncapped viral transcripts and cellular IRESes are efficiently translated, while the translation of the majority of capped cellular transcripts is inhibited. eIF4G cleavage in apoptosis is different, but again generating fragments that

appear to stimulate the expression of specific transcripts, while inhibiting general translation (Clemens, Bushell, and Morley, 1998; Henis-Korenblit, Shani, et al, 2002; Marissen, and Lloyd, 1998; Morley, McKendrick, and Bushell, 1998; Nevins, Harder, et al, 2003; Stoneley, Chappell, et al, 2000).

As a result of cellular stress conditions, the protein synthesis machinery undergoes modifications to inhibit general protein synthesis, and promote selective translation of specific transcripts. These transcripts include the previously described IRES elements, due to their lack of reliance on the mRNA cap and cap-binding protein. A specific example of the switch to IRES-mediated translation initiation has been described during hypoxia (Braunstein, Karpisheva, et al, 2007). In small tumours, cap-dependent translation is prevalent, but as the tumours increase in size and hypoxic conditions prevail, IRES-dependent translation becomes more prominent. 4E-BP levels increased with tumour size, as do levels of eIF4G. This creates an environment conducive to the IRES-mediated expression of at least three proteins important to tumour growth and survival (VEGF-A, Bcl-2 and HIF1α). This switch to cap-independent translation has been observed in a few other models as well, including heat shock, differentiation, mitosis and, as described previously, apoptosis (reviewed in Spriggs, Stoneley, et al, 2008).

In this switch to IRES-mediated protein expression, both pro-apoptotic factors important to the cell death program (such as Apaf-1 and p53) and anti-apoptotic factors critical to its counteraction are expressed. Translation of many anti-apoptotic proteins (such as Bag-1, Bcl-xL, Bcl-2, cIAP1 and XIAP) can be maintained despite global translation attenuation through the actions of their IRESes (reviewed in Graber, and Holcik, 2007).

1.5 Translational Regulation of XIAP

As mentioned previously, the 5'UTR of XIAP contains a well-studied IRES. The XIAP IRES relies on many ITAFs for its function, including La autoantigen and hnRNP C1/C2 (Holcik, and Korneluk, 2000; Holcik, Gordon, and Korneluk, 2003). The ITAFs hnRNPA1 and PTB have been found to exert an inhibitory influence on XIAP IRES activity (Baird, Lewis, et al, 2007; Lewis, Veyrier, et al, 2007).

IRES-mediated XIAP translation has been linked to X-linked dyskeratosis congenita (X-DC), a human disease characterized by bone marrow abnormalities and a predisposition to cancer (Yoon, Peng, et al, 2006). The causative gene of X-DC is *DKC1*, which encodes dyskerin, a pseudouridine synthase. As dyskerin has been known to modify ribosomal RNA, an unbiased proteomics approach was used to determine the effect of a DKC1 hypomorphic mutation on general and specific protein production. Only three proteins were found to be downregulated – all of which utilise IRES-mediated translation (p27(Kip1), Bcl-xL and XIAP). Interestingly, all clinical manifestations of X-DC can be explained through the downregulation of these three proteins. This study was the first to directly show the specific importance of cellular IRES translation *in vivo*, and provided the first knowledge of specific ribosomal alterations important to IRES-mediated translation. This hints at a possible common mechanism of ribosome recruitment for at least these three IRESes, although it remains to be seen how widespread this is.

The XIAP IRES can be activated in the response to numerous cellular stresses, including gamma irradiation, serum deprivation, and anoxia (Holcik, Lefebvre, et al, 1999; Holcik, Yeh, et al, 2000; Nevins, Harder, et al, 2003). The increased levels of XIAP after gamma irradiation and serum deprivation correlated to increased cell survival. Numerous further experiments have revealed the protective effects of XIAP in diverse cell types under various stress conditions, such as: stimulation of low potassium-induced apoptosis in

cerebral granule cells, treatment of oligodendria with staurosporine and dopamine and even ischemia/reperfusion in cardiac cells (Lyn, Bao, et al, 2002; Scarabelli, Stephanou, et al, 2004; Simons, Beinroth, et al, 1999).

It is clear that XIAP plays a critical role in the prevention of apoptosis initiated in many different ways. This has been confirmed by many studies that report its dysregulation in neurodegenerative diseases and other conditions characterized by inappropriate cell death: Huntington's disease, exaggerated death of islet cells following transplant, focal ischemia, and amyotrophic lateral sclerosis (Emamaullee, Rajotte, et al, 2005; Goffredo, Rigamonti, et al, 2005; Rami, Agarwal, and Spahn, 2007; Tokuda, Ono, et al, 2007). The problem with overexpressing XIAP in these diseases is the risk of creating cells with a propensity to stay alive longer than they should, allowing time for tumourigenic mutations to occur. It is clear that XIAP levels need to be tightly controlled, as there is a fine line between protecting cells in stress, and preventing cell death inappropriately. This has been demonstrated by the strengthening link between XIAP deregulation and cancer. High XIAP levels are common in many types of cancers, and are associated with poor prognoses (Tamm, Kornblau, et al, 2000). Some recent lines of research have focused on inhibiting XIAP protein using small molecules or anti-sense RNA (Dean, Jodrell, et al, 2009; Hao, Li, and Lu, 2007; Karikari, Roy, et al, 2007; Shaw, Lacasse, et al, 2008; Tamm, 2008). A foreseeable problem with this approach is that it is not targeted to the cancer cells. If XIAP is inhibited in all of the cells in the body, they may be less able to adapt to stresses, especially those induced by chemotherapeutics and radiation therapy. This predicted difficulty is made concrete by the existence of X-linked lymphoproliferative syndrome (XLP) (Rigaud, Fondaneche, et al, 2006). XLP can be caused by mutations in the XIAP gene, which results in a lack of XIAP protein throughout the body. The immune system is the most strongly affected, with a significant

depletion of natural killer T-lymphocytes and a lowering in the apoptotic threshold of all T cells and B cells. XLP is characterized by the increased likelihood of infections and lymphomas as a result of immune dysfunction. This data argues that total removal of XIAP is a treatment that risks many complications.

Examination of the EST database suggests of a possible approach to allow for treatment specificity. An additional XIAP mRNA isoform has been identified, sharing a completely conserved XIAP coding region and 3'UTR, as well as the 34 nucleotides immediately upstream of the start codon. (Gu, Zhu, et al, 2009; Van Eden, Byrd, et al, 2004a). The previously studied isoform has a 5'UTR spanning over 1700 nt (hereafter referred to as the Long UTR), with the IRES residing in the 3'most 162nt; the 5'UTR of the EST isoform (hereafter referred to as the Short UTR) spans only 323 nt (Holcik, Lefebvre, et al, 1999; Pruitt, Tatusova, and Maglott, 2007). Figure 3 depicts a schematic of the genomic organization of these mRNA isoforms.

Protein regulation by alternate transcripts is a widely conserved mechanism, found to play a role in development and in many cellular stress responses (Araud, Genolet, et al, 2007; Jitrapakdee, Gong, et al, 1998; McDade, Hall, and Russell, 2007). It appears that XIAP could be subject to this form of regulation, in addition to the translational control already imposed by its IRES element. If the Long and Short isoforms are differently regulated under cellular stress conditions, they could have differential importance in tumour cells versus normal cells.

My research centres on characterizing the two XIAP mRNA isoforms, with a specific focus on their expression and translational capacity in unstressed and stressed cells. I hypothesize that the two isoforms have distinct regulatory regions, and thus are regulated differently under distinct cell growth conditions.

Figure 3: The two variants of the Human XIAP mRNA.
The XIAP gene is located on the X chromosome, at the Xq25 locus. Two XIAP transcripts have been identified. The transcripts share an identical coding region and 3' UTR (not shown here), but differ in the 5'untranslated region. An internal ribosome entry site, or IRES, has been previously found in the Long UTR (Holcik, Lefebvre, et al, 1999). Genomic sequence is shown in solid blue, introns are indicated by a dotted line, exons are shown in grey and the arrow above "AUG" indicates the location of the start codon.

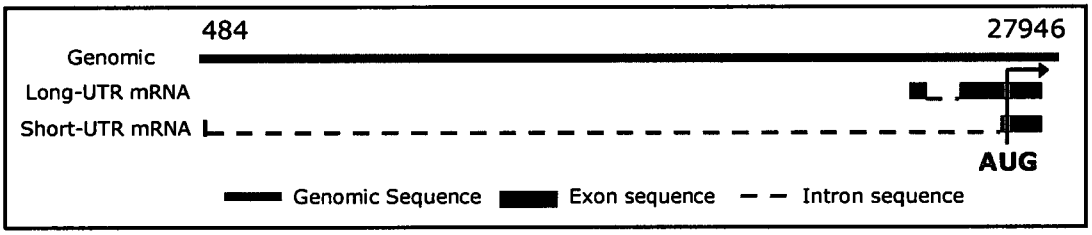
484
27946
Genomic
Long-UTR mRNA
Short-UTR mRNA
AUG
Genomic Sequence
Exon sequence
Intron sequence

Identification of the cellular role for each transcript will provide specific knowledge regarding the tight translational control of XIAP expression, as well as general knowledge of a potentially widespread protein regulation mechanism through alternate transcripts.

Chapter 2: Materials & Methods

2.1 Reporter construct preparation

Bic-Long (full-length Long UTR), mono-Long, Bic-Short (full length Short UTR), and mono-Short were previously prepared in the laboratory (Baird, Lewis, et al, 2007; Holcik, Lefebvre, et al, 1999). Subsequently, I created the following constructs: Bic Long-170, Bic Long-350, mono Long-170, mono Long-350, all of the hairpin constructs and all of the synthetic RNAs. All bicistronic constructs were in the vector pBicmod, and all monocistronic constructs were in the vector pCAT (identical to pBicmod, without the βgal gene) (Baird, Lewis, et al, 2007). Appendix I shows a representative construct, Bic-Long. The pBicmod vector is based on the pcDNA3 cloning vector (Invitrogen). All oligonucleotides used in all protocols were obtained from Invitrogen, oligonucleotide sequences can be found in Appendix II. Exceptions are the Long UTR siRNA (XIAP IRES 751), and the Quantitect qXIAP, qEEF1A1, q4496 and q323 primers, which were ordered from Qiagen.

Polymerase Chain Reaction (PCR)-amplified sequence from the full-length Long UTR-containing construct was analyzed by agarose gel electrophoresis to confirm the presence and correct size of inserts (Primers: 4571NheI-F (for Long-170) or 350NheI-F and 4405XhoI-R). TOPO TA cloning (Invitrogen) was used to insert UTR sequence into the pCR 2.1 vector, followed by EcoRI digest of miniprep DNA to identify UTR-positive clones. The UTRs were then ligated into the Bic-empty plasmid (NheI, XhoI (Invitrogen)). After purification, insert presence was confirmed (NheI, XhoI digest), and constructs were sequenced. Monocistronic constructs were prepared from the bicistronic constructs by digestion with NotI (Invitrogen) to remove the βgal gene, and self-ligation to recreate the circular vector. The monocistronic construct was then transformed into Invitrogen DH5α *E. coli* cells. To obtain pure preparations of the

monocistronic and bicistronic constructs from DH5α, the Qiagen Maxiprep kit was used according to the manufacturer's protocol. Constructs were confirmed by NheI/XhoI digest, which liberated the inserts.

Hairpin constructs were created by insertion of a double stranded sequence containing an internal PmeI site into the NheI site immediately 5' of the UTR in each construct. This hairpin element was created by annealing oligonucleotides BCHP-1 and BCHP-2 (sequence in Appendix II, structure in Appendix I). To verify presence of the hairpin, the vectors were digested with PmeI and XhoI to excise the hairpin + UTR, and visualized on a 1.2% agarose gel. All constructs were eventually transformed into DH5α cells, and it is from these cultures that the purified constructs were obtained (Qiagen CompactPrep Plasmid Maxi kit). DNA concentration determinations of all purified constructs were done using the ND-1000 spectrophotometer (NanoDrop technologies). A schematic of all representative transcripts resulting from transfection of these constructs is seen in Figure 4.

2.2 Synthetic RNA preparation

PCR was used to create templates for *in vitro* transcription of RNA for transfection. The forward primer included the full T7 sequence to allow for RNA transcription and the reverse primer included the 3' end of the CAT gene, as well as 31 Ts, which were added to the end of the PCR product to provide polyA tail. PCR was performed, using mono-Empty (+/-HP), mono Long-350 (+/-HP) or mono Short-323 (+/-HP) as templates. The PCR products were purified by agarose gel electrophoresis. *In vitro* transcription and capping was performed with the Ambion mMessage mMachine kit, as per the manufacturer's protocol, and the newly synthesized RNA was purified using a

Figure 4: The reporter mRNA.
Schematic diagram of the monocistronic, monocistronicHP, bicistronicHP, monocistronic IVT RNA and monocistronicHP IVT RNA reporter mRNAs that were used throughout the study. Schematic legend: mRNA cap (grey), +/- hairpin (black), βgal cistron (blue), UTR (black), CAT cistron (green).

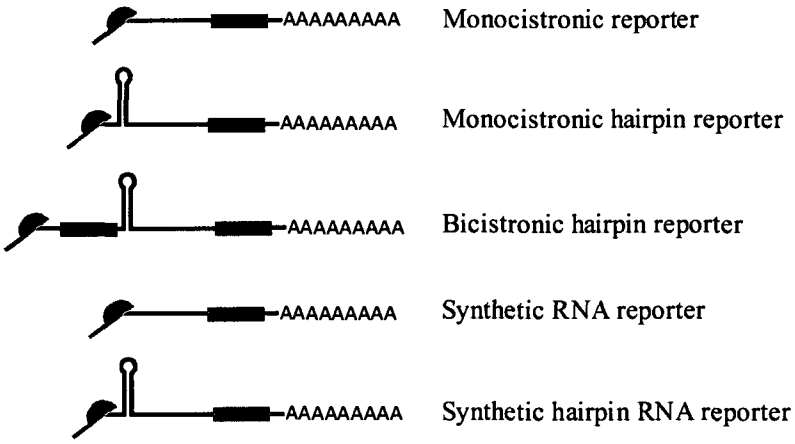
AAAAAAAAA
Monocistronic reporter
AAAAAAAAA
Monocistronic hairpin reporter
AAAAAAAAA
Bicistronic hairpin reporter
AAAAAAAAA
Synthetic RNA reporter
AAAAAAAAA
Synthetic hairpin RNA reporter
7-methylguanosine cap
βgal cistron
CAT cistron
Hairpin element

Megaclear column (Ambion). The concentration of the resulting RNA (capped, with a poly(A) tail) was determined using the ND-1000 spectrophotometer (NanoDrop technologies). Prior to transfection, a small volume of RNA was analyzed. The secondary structure of each RNA was melted at 60°C and agarose gel electophoresis was used to confirm the size of the transcripts. Representative synthetic mRNAs are depicted in Figure 4.

2.3 Cell Culture and Transfection

HEK293 cells were maintained at 37°C, 5% CO_2 in complete DMEM (1% FBS, 1% glutamine, 100,000 U/L penicillin, 100 µg/L streptomycin) (Wisent, Inc.).

Human keratinocyte HF1-E cells (kindly provided by Dr. Alexander Levitzki) were maintained at 37°C, 5% CO_2 in KGM media (DMEM, 25% Nutrient mixture F-12 (HAM), 10% fetal bovine serum, 5 µg/ml insulin, 0.4 µg/ml hydrocortisone, 10^{-10} M cholera toxin, 10 ng/ml epidermal growth factor, 1.8×10^{-4} M adenine, 5 µg/ml transferrin, 2×10^{-9} M T3, 100,000 U/L penicillin, 100 µg/L streptomycin).

All other cell lines were obtained in confluent 10 cm dishes from Dr. Herman Cheung (A375, ACHN, Capan-2, HeLa, MCF-7, SK-N-AS, SK-N-BE(2) and U2OS), and were immediately harvested in RNA lysis buffer (0.3M NaCl, 15mM $MgCl_2$, 15mM Tris pH 7.4, 1% Triton X, 0.0025% RNasin, 0.1mg/ml cycloheximide).

For DNA transfections, HEK293 cells were seeded 24 hours prior to transfection at ~$3x10^5$ cells/2 ml/well (Corning 6-well plate coated with poly-D Lysine). Transient transfections of 1.5 µg construct DNA per well were performed using Lipofectamine™ 2000 (Invitrogen). Cells harvested 48 hrs later in CAT Lysis Buffer (Roche) for protein quantification, or in Stratagene Lysis Buffer for RNA quantification.

For synthetic RNA transfections, HEK293 cells were seeded 24 hours prior to transfection at ~$3x10^5$ cells/ml/well in a 12-well plate (Corning). Transient transfections of 1 μg synthetic RNA per well were performed using Lipofectamine™ 2000 (Invitrogen). Cells were harvested 4 hrs later in CAT Lysis Buffer (Roche) for protein quantification, or in Stratagene Lysis Buffer for RNA quantification.

For siRNA experiments, double stranded siRNAs targeting the Long UTR (XIAP IRES 751,Qiagen) or the Short UTR (stealth 62 and 172, Invitrogen) were designed, and non-targeting siRNA was used as a negative control (Qiagen). As a positive control, SMARTpool siRNA targeting the 3'UTR of XIAP was used (Dharmacon). HEK293 cells were plated as for DNA transfections. The cells were transfected for ~24-48 hrs with 20nM siRNA, using DharmaFECT™ 1 (Dharmacon). 48 hours later, cells were harvested in radioimmunoprecipitation assay (RIPA) buffer for protein determination or for RNA in Stratagene Lysis Buffer.

For the serum deprivation experiments in HEK293 cells, 24 to 48 hours after siRNA transfection or 24 hours after cell seeding for untransfected cells, the media was removed from the well, and each well was carefully rinsed with warm phosphate-buffered saline (PBS). To the control wells, complete DMEM was added to each well, while DMEM containing only glutamine, penicillin and streptomycin was added to the wells to be serum starved. For polysome profiling, this took place in 15 cm dishes. After 24 to 48 hours, media was removed, and cells were harvested in RIPA buffer for protein quantification, or in CHX RNA Lysis Buffer (0.3M NaCl, 15mM $MgCl_2$, 15mM Tris pH 7.4, 1% Triton-X100, 100U/ml RNAsin, 0.1mg/ml Cycloheximide (CHX)) for Polysome Profiling.

For the rapamycin experiments, HF1-E cells were seeded 1:2 in 6 well plates (for Western Blotting) or 15 cm plates (for polysome profiling) in KGM media. When cells

had reached ~60-75% confluency (~24 hrs), Rapamycin (Sigma-Aldrich, in DMSO) was added to the cells at a concentration of 150 nM. To untreated cells, equivalent amounts of DMSO were added. After 24 hours, cells were harvested in RIPA buffer for protein determination or CHX RNA Lysis Buffer for Polysome Profiling. Due to strong adherence of cells to the dish, cells were scraped directly into the buffers.

2.4 βgal, CAT and Neo assays

Cell lysates in CAT lysis buffer (Roche) were tested in three different assays following centrifugation to remove cell debris (Hettich temperature-controlled benchtop centrifuge). The βgalactosidase (βgal) assay was performed in a Corning 96 well plate in Z buffer (60 mM Na_2PO_4, 40 mM NaH_2PO_4, 10 mM KCl, 1 mM $MgSO_4$, 50 mM B-mercaptoethanol, pH 7.0) using ONPG (4 mg/ml in 0.1 M NaP buffer, pH 7.5) as a colorimetric substrate (MacGregor, Nolan, et al, 1991). The reaction was stopped with Na_2CO_3, and the absorbance was read at 420 nm. The chloramphenicol acetyltransferase (CAT) ELISA (Roche) and neomycin phosphotransferase II (Neo) ELISA (Agdia) were performed and the results measured according to the manufacturer's protocol, using a Spectramax 340PC plate reader (Molecular devices).

2.5 RNA Extraction and PCR

RNA purification was performed using the Absolutely RNA® Miniprep kit as per manufacturer's instructions (Qiagen RNeasy Mini Kit for cell line screen) and reverse transcription (RT) was performed using the GE Healthcare First Strand cDNA Synthesis Kit (NotI-$(dT)_{18}$ RT primer for plasmid-and IVT RNA-transfected cells, $pd(N)_6$ RT primer for others). qRT-PCR was performed using SYBR green Master Mix (Qiagen) (Primers: qCAT F&R, qNeo F&R, qGAL F&R for plasmid-transfected

cells, CAT F&R for IVT RNA-transfected cells, Quantitect qXIAP, q4496 F&R, q323 F&R and qActin F&R for endogenous mRNA quantification).

qRT-PCR was performed using the 7000 Sequence Detection System and its associated software (Applied Biosystems) for the cell line screen; the Stratagene Mx3005P™ and its associated software (Mx Pro™) was used for all other qPCR. Cycling conditions: 95°C for 15min, 94°C for 15s, 55°C for 30s, 72°C for 30s, 40cycles. Dissociation curves were also obtained: 95°C for 15s 60°C for 20s, 95°C for 15s.

Semi-quantitative PCR was performed using Taq polymerase (Invitrogen) in DNA Engine Dyad® Peltier Thermal cycler (MJ Research) and PCR products were resolved on a 1.5% agarose gel, visualized with EtBr, and quantified using Odyssey densitometry software (Licor). Primers used: CHEOXIRES F (L1), REFSEQXUTR F (S1), XIAP CDS F&R (C1&C2), qGAPDH F&R, Quantitect EEF1A1, qCAT F&R. Cycling conditions: 95°C for 5min, 94°C for 30s, 54°C for 50s, 72°C for 120s, 18-35 cycles.

The RT-PCR efficiency controls were done by performing PCR directly on construct DNA (mono-Long and mono-Short), or on cDNA obtained from synthetic Long and Short UTR-containing RNA. Primers used: CHEOXIRES F, REFSEQXUTR F, CAT F&R.

2.6 Western Blotting

Protein levels were assessed by sodium dodecyl sulfate-polyacrylamide gel electrophoresis (SDS-PAGE) and subsequent protein detection by antibody (Western blot). Cells were harvested in ice cold PBS, and centrifuged to remove debris. The cell pellet was lysed in radioimmunoprecipitation assay (RIPA) buffer (50mM Tris Cl pH7.4, 1mM EDTA, 150mM NaCl, 1% NP40, 0.5% Deoxycholic acid, 0.05% SDS) with the addition of protease inhibitors (1 μM leupeptin, 1 mM PMSF). When

phospho-rpS6 levels were being queried, phosphatase inhibitors were included in the RIPA buffer (50uM NaF, 5uM β-glycerol phosphate). The cells were lysed for 30 minutes in a rotator at room temperature, followed by centrifugation at 12000 rpm in a 4°C bench top centrifuge (Hettich). The supernatant was collected, and Bradford-Lowry Assays were used to determine protein concentration (BioRad). Equal protein amounts (20-40 μg) were diluted in Laemmli Buffer, 5% β-mercaptoethanol (Sigma-Aldrich) and loaded on 10% acrylamide gel and SDS-PAGE was performed. Following electrophoresis, the proteins were transferred to a PVDF membrane using semi-dry transfer (90 min at 60mA), or to a nitrocellulose membrane using wet transfer (1 hr at 110V). The levels of the following proteins were queried: XIAP (rabbit αRIAP3 antibody, 1:5000 in 1% milk PBST (Holcik, Lefebvre, et al, 2002), mouse αGAPDH (1:20 000 in 1% milk PBST, Advanced Immunochemical), mouse αActin (1:10 000 in 1% milk PBST, Sigma), mouse αrpS6 (1:1000 in 5% milk TBST, Cell Signalling Technology), rabbit αP-rpS6 (Ser 240, 244, 1:2000 in 5% BSA TBST, Cell Signalling Technology). Secondary antibodies used were α-rabbit or α-mouse (1:5000-1:10 000, BioRad). ECL and ECL plus (GE Healthcare) as well as West PICO substrates (Pierce) were used to visualize protein on Hyperfilm (GE Healthcare).

2.7 Polysome Profiling

HEK293 or HF1-E cells from between three and six 15cm plates per condition were pooled in CHX RNA lysis buffer (0.3M NaCl, 15mM $MgCl_2$, 15mM Tris pH 7.4, 1% Triton-X100, 100U/ml RNAsin, 0.1mg/ml CHX), and lysed for 30 min. Nuclei were pelleted by centrifugation at 5000 rpm, and the supernatant was spun at 13000rpm to remove cellular debris. Up to 800μl of supernatant was carefully added on top of a 10%-50% sucrose gradient column, while reserving at least 200 μl for total RNA analysis. The

columns were centrifuged for 90 minutes at 35000 rpm (4°C) in SW41Ti rotor (average force approximately equal to 188 000 x g) in an Optima L-100 xP Ultracentrifuge (Beckman Coulter). Following centrifugation, the samples were fractionated using an Auto densi-flow (Labconco) and ÄKTA Explorer FPLC, with UV900 and P900 modules (Amersham Pharmacia biotech) and the associated Unicorn 4.11 Software (Amersham). Fractionation was done in 1 ml (monosome fractions) or 0.5 ml fractions (polysome fractions), in accordance with the UV absorbance representing the monosomal and polysomal fractions. Fractions were flash-frozen in dry ice and stored at -80°C. After thawing on ice, the fractions were spiked with 10 µl of a 10 ng/µl solution of *in vitro*-transcribed CAT RNA, to ensure technical consistency in RNA extraction. Fractions were heated for 1 hr after addition of 50 µl Extraction Master Mix per ml (37.5µL 10% SDS, 7.5 µL 0.5M EDTA, 1 µL Glycoblue (Ambion), 3.75 µL 20mg/ml Proteinase K) and RNA was extracted using phenol/chloroform/isoamyl alcohol and chloroform (Sigma). RNA was recovered by ethanol precipitation, RT and PCR as described in RNA Extraction and PCR. Primers: CHEOXIRES F, REFSEQXUTR F, XIAP CDS F&R, qGAPDH F&R and CAT F&R.

2.8 Primer Design

All primer sequences can be found in Appendix II. I designed all primers, with the following exceptions.

CHEOXIRES F, REFSEQXUTR F, XIAP CDS F&R– kindly provided by Dr. Stephen Baird.

T7 F, NT4 – kindly provided by Dr. Nehal Thakor.

BCHP-1, BCHP-2 – kindly provided by Dr. Martin Holcik.

EEF1A1 Quantitect Primer Assay, qXIAP Quantitect Primer Assay, q4496, q323 – designed by Qiagen.

qCAT F&R, qGAL F&R, qNeo F&R, qGAPDH F&R,– kindly provided by Tyson Graber.

qActin F&R – sequences kindly provided by Dr. John Bell.

2.9 Statistical Analysis

Data are expressed as mean +/- standard deviation. Unless otherwise stated, all results reported here were obtained through a minimum three independent experimental replications. For all reporter assays, each independent replicate consisted of biological triplicates. Unpaired t-tests were used to determine data significance.

Chapter 3: Results

3.1 Both XIAP mRNA isoforms exist in many cell types and the Short variant is more abundant than the Long variant.

The anti-apoptotic protein XIAP has been studied extensively, as its dysregulation plays a role in many human diseases (reviewed in Lotocki, and Keane, 2002). The XIAP mRNA was found to contain an internal ribosome entry site or IRES, which protects cells from apoptotic death (Holcik, Lefebvre, et al, 1999). This transcript, especially its IRES, was the subject of many subsequent studies (Gu, Zhu, et al, 2009; Holcik, Yeh, et al, 2000; Holcik, Gordon, and Korneluk, 2003; Lewis, and Holcik, 2005; Lewis, Veyrier, et al, 2007; Spahn, Blondeau, et al, 2008; Yoon, Peng, et al, 2006). In a 2004 paper by Van Eden *et al.*, the existence of this transcript was called into question (Van Eden, Byrd, et al, 2004a). This same paper described a different XIAP mRNA isoform identified through scanning of the expressed sequence tag (EST) database, although its *in vivo* relevance has not been examined. The two identified isoforms share identical XIAP coding regions and 3'UTRs; however, their 5'UTRs (barring the 30 nt immediately upstream of the start codon) are mutually exclusive. The organization of both XIAP mRNA isoforms with respect to the X chromosome and each other is depicted in Figure 3.

Semi-quantitative multiplex PCR was used to analyze the expression pattern and abundance of both XIAP mRNA isoforms in a panel of ten different cell lines (Figure 5). Both mRNA isoforms could be detected in all cell lines tested. It was noted that the relative intensity of the bands representing each transcript was fairly consistent over the cell line panel. The band representing the Short mRNA isoform is always much more intense than the band representing the Long variant. To ascertain if the multiplexing of the PCR was having a confounding effect on the apparent results, each primer set was

Figure 5: Both XIAP mRNA variants are present in human cell lines.
(A) A schematic of the specific primers designed to amplify each UTR and the XIAP coding region. The primers were designed such that the PCR product specific to each mRNA isoform also overlapped the XIAP coding region. Primers used: Long: L1(CHEOXIRES F) & C2 (XIAPCDS R), Short: S1 (REFQXUTR F) & C2(XIAPCDS R), Coding: C1 (XIAPCDS F) & C2(XIAPCDS R),.
(B) A panel of diverse cell lines was probed for the two XIAP isoforms. RNA was extracted from each cell line, followed by reverse transcription with a random hexamer RT primer, PCR using the primers described in (A) and agarose gel electrophoresis. Templates for PCR were cDNA derived from: 1:SKMEL5, 2:SK-N-BE(2), 3:SK-N-AS, 4:A375, 5:HeLa, 6:Capan-2, 7:U2OS, 8:ACHN, 9:MCF-7, 10:HEK293. The template used in lane 11 was RNA extracted from HEK293 cells (no RT reaction was performed). Long marks the band representing the Long XIAP isoform, Short marks the band representing the Short XIAP isoform, and Coding marks the band representing the XIAP coding sequence.

A

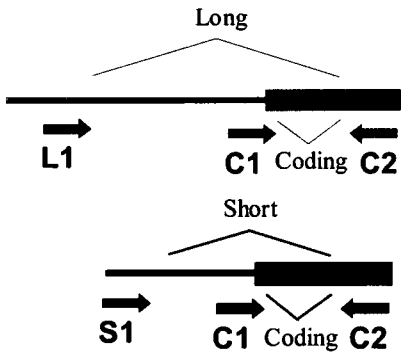
Long
L1
C1
Coding
C2
Short
S1
C1
Coding
C2

B

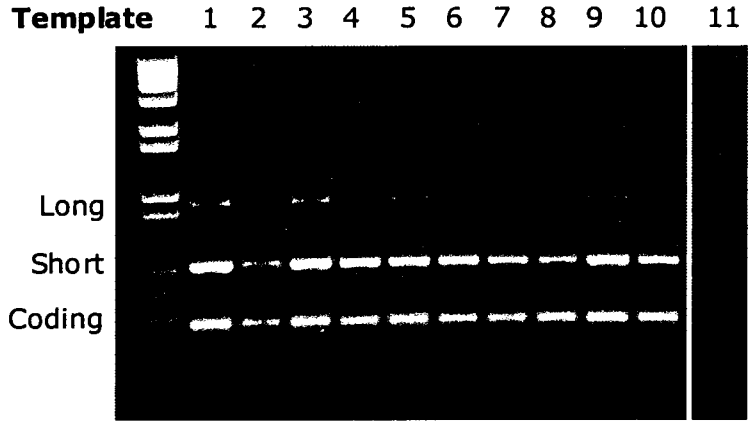
Template
1
2
3
4
5
6
7
8
9
10
11
Long
Short
Coding

used in isolation (Figure 6A). The relative band intensities were virtually identical to those observed in the multiplex PCR experiments. To ensure that the PCR or reverse transcription did not have differing efficiencies on each transcript, the following control experiments were performed. To test for primer efficiency, PCR was carried out on cloned DNA for each XIAP isoform (Figure 6B). The equivalent band intensities indicate the equal efficiencies of the PCR primers for both isoforms. To rule out differently efficient reverse transcription due to structural and sequence differences between the two XIAP isoforms, RT-PCR was performed using *in vitro*-synthesized RNA as a template (Figure 6C). As the same pattern was again observed, it can be concluded that the relative transcript abundance indicated by semi-quantitative PCR is correct; the Long XIAP isoform is present at much lower levels than the Short isoform.

3.2 The Long XIAP mRNA isoform contains an IRES and does not facilitate cap-dependent translation initiation.

On examination of the isoform sequences, it was noted that they only differ in a regulatory region – the 5'UTR. This suggests that the distinct UTRs might play a role in the translational control of XIAP protein.

To facilitate the translational characterization of each XIAP isoform, a set of reporter constructs was generated. Each full UTR[1] was cloned into monocistronic (pCAT) and bicistronic (pBicmod) reporter plasmids. A schematic of all construct types used can be found in the Methods section (Figure 4). Transient transfections with these constructs were carried out in HEK293 cells, and the amount of each reporter gene product present was determined using enzyme activity assays (for β-galactosidase or

[1] Only the 3' 1kb portion of the Long UTR is available, so this will constitute the "full-length UTR" sequence in the constructs for these experiments.

Figure 6: The Short XIAP isoform is more abundant than the Long isoform.
(A) The primer sets depicted in Figure 5 were tested in isolation on SK-N-AS cDNA obtained as described in Figure 5B to compare the amplification observed with each primer set separately. Primers used: 1 – C1 & C2, 2 – L1 & C2, 3 – S1 &C2. Lane 4 was primers C1 & C2, using RNA extracted from SK-N-AS cells (no RT) as a template.
(B) PCR was performed as in (A), using a monocistronic DNA construct containing either the Long or Short UTR as a template. In place of the XIAP coding primers, primers specific to the CAT coding sequence were used (qCAT F & R). 1 – Primers: L1 & CAT R, Template: Long; 2 – Primers: CAT F & CAT R, Template: Long; 3 – Primers: S1 & CAT R, Template: Short; 4 – Primers: CAT F & CAT R, Template: Short.
(C) PCR was performed as in (B), using equal amounts of cDNA template reverse transcribed from synthetic RNA containing the CAT coding sequence and one or the other of the UTR sequences. 1 – Primers: L1 & CAT R, Template: Long; 2 – Primers: CAT F & CAT R, Template: Long; 3 – Primers: S1 & CAT R, Template: Short; 4 – Primers: CAT F & CAT R, Template: Short.

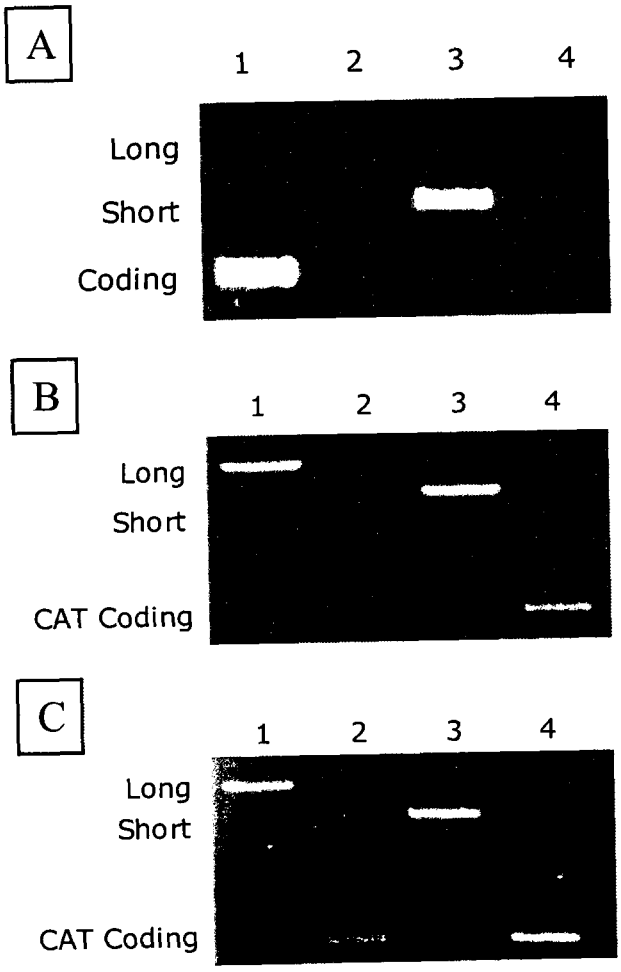
A
1
2
3
4
Long
Short
Coding
B
1
2
3
4
Long
Short
CAT Coding
C
1
2
3
4
Long
Short
CAT Coding

βgal) and enzyme-linked immunosorbent assays (ELISAs) for chloramphenicol acetyltransferase (CAT) and neomycin phosphotransferase II (Neo). The monocistronic assays provide information about the influence of the 5'UTR sequence on cap-dependent translation, while the bicistronic assays provide information about cap-independent, IRES-dependent translation.

The *ex vivo* monocistronic construct assay in HEK293 cells revealed the effect of the Long XIAP UTR on translation of a downstream cistron (See Figure 7). The construct expresses a capped and polyadenylated transcript coding for CAT, which is under the translational control of the UTR of interest, inserted immediately upstream of the CAT coding sequence. This construct also expresses a Neo transcript, which, since driven by a separate promoter, can be used as a control for efficiency of transfection. The Neo- and RNA-normalized levels of CAT protein represent the amount of CAT protein being produced per amount of RNA. In comparison with the empty monocistronic vector, the vector containing the Long XIAP UTR produces the same amount of protein per RNA. This level of translation remains unchanged if only the 3'most 162 nt (minimal IRES (Holcik, Lefebvre, et al, 1999)) are included in the construct. This indicates that the Long XIAP 5'UTR does not exhibit a repressive effect on translation of a downstream cistron in a cap-dependent context.

To examine the IRES activity of the Long UTR, a bicistronic construct was developed to express a capped and polyadenylated transcript, containing the βgal gene, a sequence coding for a hairpin structure, the Long UTR, and the CAT coding sequence (Figure 8). Since βgal protein levels represent the level of cap-dependent translation, CAT protein levels normalized to βgal expression represent the level of relative IRES-dependent translation initiation. This follows from the fact that in the mammalian system, ribosomes usually dissociate from a transcript upon reaching a stop codon and do not

Figure 7: The Long XIAP UTR has no effect on translation of a downstream cistron.
(A) Depicted are the transcripts resulting from transfection of monocistronic constructs. These constructs were used to examine translational effects of the Long UTR. The constructs were created from the pBicmod vector. Expression of the monocistronic CAT transcript is driven by the CMV promoter. Expression of a Neo transcript elsewhere on the plasmid is driven by the SV40 promoter, allowing normalization of the expressed CAT values to transfection levels.
(B) HEK293 cells in 6 well plates were transfected with 1.5μg monocistronic construct DNA, using Lipofectamine™ 2000. Cells were lysed after 48 hours, and ELISA methods were used to quantify CAT and Neo protein levels. In parallel to lysis for ELISA, RNA was extracted and reverse transcription was performed. Quantitative RT-PCR was performed using qCAT and qNeo primers; results obtained through ΔΔct method. Results shown as CAT to Neo protein, normalized to CAT to Neo RNA. Empty set to 1.

A

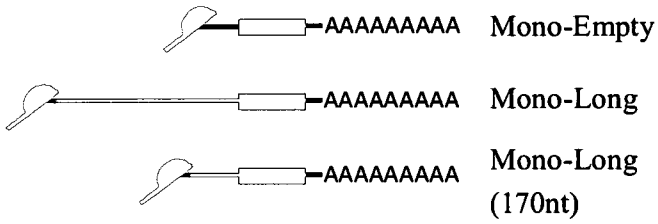
AAAAAAAAA
Mono-Empty
AAAAAAAAA
Mono-Long
AAAAAAAAA
Mono-Long
(170nt)

B

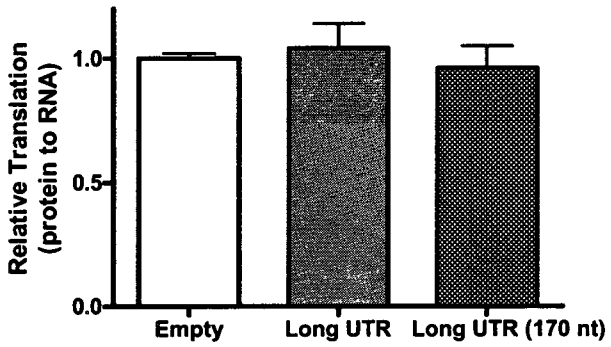
Relative Translation
(protein to RNA)
1.0
0.5
0.0
Empty
Long UTR
Long UTR (170 nt)

Figure 8: The Long XIAP UTR has an internal ribosome entry site, and is not dependent on ribosomal scanning for translation.
(A) HEK293 cells in 6 well plates were transfected with 1.5μg bicistronic construct DNA, using Lipofectamine™ 2000. Cells were lysed after 48 hours; βgal levels were determined through an enzymatic activity assay, while CAT levels were quantified using ELISA. Results shown as CAT protein normalized to βgal protein. Empty set to 1.
(B) HEK293 cells in 6 well plates were transfected with 1.5μg monocistronic (plus/minus hairpin) construct DNA, using Lipofectamine™ 2000. Cells were lysed after 48 hours, and ELISA methods were used to quantify CAT and Neo protein levels. In parallel to lysis for ELISA, RNA was extracted and reverse transcription was performed. Quantitative RT-PCR was performed using qCAT and qNeo primers; results obtained through ΔΔct method. Results shown as CAT to Neo protein, normalized to CAT to Neo RNA. Minus hairpin set to 1.

A

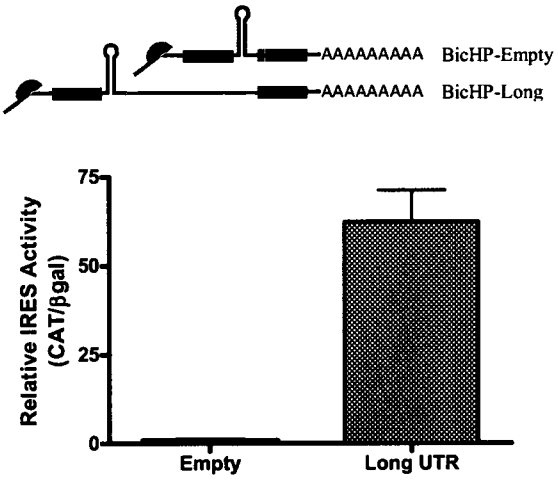
AAAAAAAAA BicHP-Empty
AAAAAAAAA BicHP-Long
Relative IRES Activity (CAT/βgal)
75
50
25
0
Empty
Long UTR

B

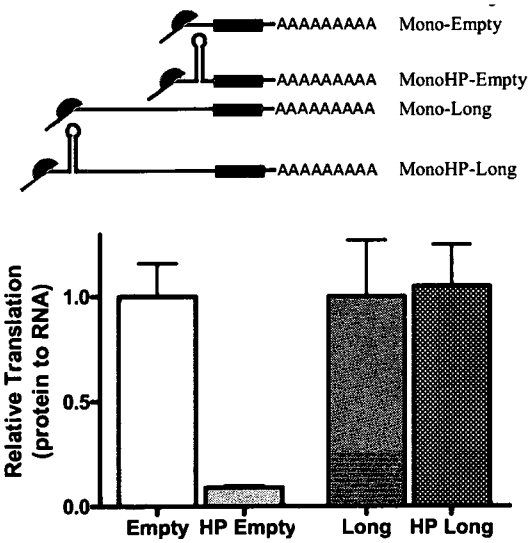
AAAAAAAAA Mono-Empty
AAAAAAAAA MonoHP-Empty
AAAAAAAAA Mono-Long
AAAAAAAAA MonoHP-Long
Relative Translation (protein to RNA)
1.0
0.5
0.0
Empty
HP Empty
Long
HP Long

efficiently re-initiate translation of subsequent open reading frame (reviewed in Hershey, 1991). Therefore, levels of CAT observed represent the result of translation that is not dependent on recruitment to the cap and subsequent scanning to the CAT start codon. However, since the bicistronic transcript is driven by a highly active CMV promoter, it is possible that enough chance events of ribosomal reinitiation may occur as to skew the results. This is why a strong (ΔG=-38 kcal/mol) hairpin structure was introduced immediately downstream of the βgal gene (see Appendix I for hairpin structure, Appendix II for sequence). This structure is expected to prevent a ribosome from scanning through, and ensures that nearly all ribosomes will dissociate from the transcript at the βgal stop codon.

HEK293 cells were transfected with 1.5 μg bicistronic construct for 48 hours in 6 well plates. Following cell lysis, levels of βgal and CAT protein were measured using an enzymatic assay and ELISA, respectively. The bicistronic assay shows a considerable increase in CAT translation when the Long UTR is inserted into the vector (Figure 8). The CAT/ βgal ratio is more than 50-fold higher than that seen for the empty vector. This indicates that the Long UTR is capable of directing high levels of translation in a method independent of scanning from the cap. In the past, the reliability of bicistronic reporter assays has been called into question (Van Eden, Byrd, et al, 2004a). It was noted that in some bicistronic constructs, splicing out of the first cistron could occur, thereby increasing the observed level of cap-independent translation. This possibility in the βgal/CAT vector was previously addressed and subsequently discounted in a study by Holcik *et al.* ((Holcik, Graber, et al, 2005). To further confirm that XIAP IRES is a *bona fide* IRES element, an alternate approach was used to assess the reliance of the observed translation on scanning from the cap. Monocistronic constructs were used (as in Figure 7), but with the addition of a strong hairpin structure (see Appendix

I) immediately 5' of the UTR (Figure 8). This hairpin is quite efficient at impeding ribosomal scanning from the cap, as evidenced by the dramatic reduction in translation of the empty control vector following hairpin insertion (Figure 8). However, the insertion of a hairpin in the Long UTR-containing vector had no effect on the expression of CAT reporter gene. This indicates that nearly all translation driven by this UTR is IRES-mediated. Although Figure 7 showed no adverse effect on translation of a downstream cistron, it appears to be because cap-dependent translation is not occurring and translation driven by the strong IRES element is taking its place. This corroborates the results of the bicistronic assay; the Long UTR is capable of efficiently driving translation initiation in the absence of ribosomal scanning from the cap.

3.3 The Short XIAP mRNA isoform does not contain an IRES and relies on inefficient cap-dependent translation.

The 5'UTR of the Short mRNA variant was placed in monocistronic (plus/minus hairpin) and bicistronic constructs; the translation of these constructs was subsequently studied in HEK293 cells.

As seen in Figure 9, the levels of CAT protein normalized to CAT RNA driven by the Short UTR are quite low in comparison to the levels driven by the empty monocistronic vector. The presence of the Short UTR reduces translation efficiency of the downstream CAT gene by more than 60%, suggesting that the Short UTR prevents efficient cap-dependent translation. To assess the putative IRES activity of the Short UTR, a bicistronic reporter assay was used (Figure 10). The protein levels produced by the Short UTR-containing bicistronic vector were examined, and found to be quite similar to those produced by the empty vector. Taking into account the variability of

Figure 9: The Short XIAP UTR has an inhibitory effect on translation of a downstream cistron.
(A) Depicted are the monocistronic transcripts resulting from transfection of monocistronic constructs. These constructs were used to examine translational effects of the short UTR and were created using the pBicmod vector. Expression of a Neo transcript elsewhere on the plasmid is driven by the SV40 promoter, which allows a normalization of the expressed CAT values to transfection efficiency.
(B) HEK293 cells in 6 well plates were transfected with 1.5μg monocistronic construct DNA, using Lipofectamine™ 2000. Cells were lysed after 48 hours, and ELISA methods were used to quantify CAT and Neo protein levels. In parallel to lysis for ELISA, RNA was extracted and reverse transcription was performed. Quantitative RT-PCR was performed using qCAT and qNeo primers; results obtained through ΔΔct method. Results shown as CAT to Neo protein, normalized to CAT to Neo RNA. Empty set to 1.

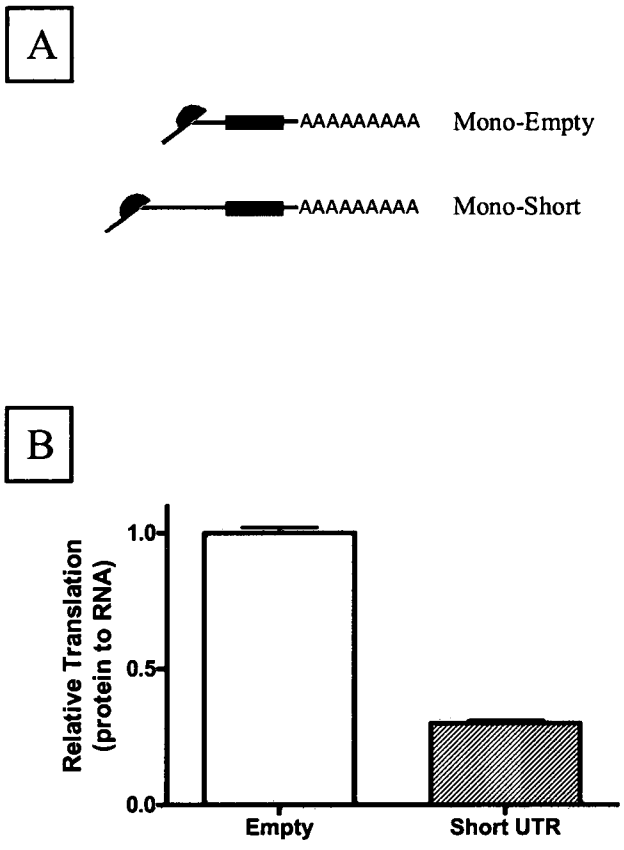
A
AAAAAAAAA
Mono-Empty
AAAAAAAAA
Mono-Short
B
Relative Translation
(protein to RNA)
1.0
0.5
0.0
Empty
Short UTR

Figure 10: The Short XIAP UTR does not have an internal ribosome entry site, and is dependent on ribosomal scanning for translation.
(A) Depicted are the bicistronic transcripts resulting from transfection of bicistronic constructs. The constructs were used to examine scanning independence and IRES activity and were derived from pBicmod. They include a strong hairpin sequence immediately 5' of the UTR. The monocistronic and monocistronic hairpin constructs are like those described in Figure 8A, but containing the Short UTR. Lack of statistical significance determined by unpaired T test ($p>0.1$)*
(B) HEK293 cells in 6 well plates were transfected with 1.5μg bicistronic construct DNA, using Lipofectamine™ 2000. Cells were lysed after 48 hours; βgal levels were determined through an enzymatic activity assay, while CAT levels were quantified using ELISA. Results shown as CAT protein normalized to βgal protein. Empty set to 1.
(C) RNA was extracted from HEK293 cells transfected as in (B) and reverse transcription was performed. Quantitative RT-PCR was performed using qCAT and qGal primers; results obtained through ΔΔct method. Results shown as CAT to βgal RNA.
(D) HEK293 cells in 6 well plates were transfected with 1.5μg monocistronic (plus/minus hairpin) construct DNA, using Lipofectamine™ 2000. Cells were lysed after 48 hours, and ELISA methods were used to quantify CAT and Neo protein levels. In parallel to lysis for ELISA, RNA was extracted and reverse transcription was performed. Quantitative RT-PCR was performed using qCAT and qNeo primers; results obtained through ΔΔct method. Results shown as CAT to Neo protein, normalized to CAT to Neo RNA. Minus hairpin set to 1.

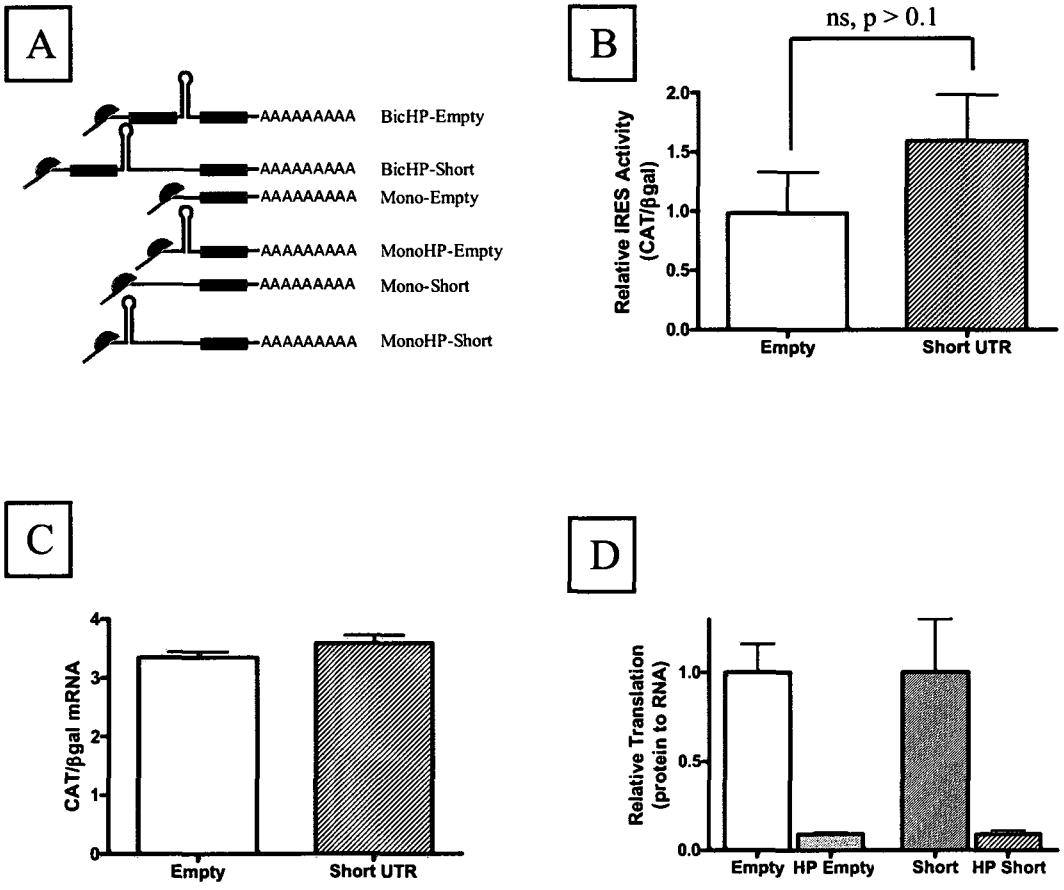
A
AAAAAAAAA
BicHP-Empty
AAAAAAAAA
BicHP-Short
AAAAAAAAA
Mono-Empty
AAAAAAAAA
MonoHP-Empty
AAAAAAAAA
Mono-Short
AAAAAAAAA
MonoHP-Short
B
ns, p > 0.1
Relative IRES Activity (CAT/βgal)
2.0
1.5
1.0
0.5
0.0
Empty
Short UTR
C
CAT/βgal mRNA
4
3
2
1
0
Empty
Short UTR
D
Relative Translation (protein to RNA)
1.0
0.5
0.0
Empty
HP Empty
Short
HP Short

the assay, the IRES-dependent translation driven by the Short UTR is essentially background ($p>0.1$, unpaired t test). To ensure that splicing of the bicistronic transcript was not skewing the observed results, quantitative Real-Time PCR was performed on RNA extracted from HEK293 cells. Levels of βgal and CAT coding RNA were quantified using this method, and it was found that the ratio of CAT cistron RNA to βgal cistron RNA obtained from cells transfected with the Short UTR-containing vector was identical to that from the empty vector (Figure 10). To address the possibility of error in the bicistronic system, an alternate approach was also used. A monocistronic hairpin construct was developed to confirm the lack of IRES activity in the Short UTR. As can be seen, the hairpin drastically diminishes the expression of the reporter gene in the empty vector (Figure 10). This is mirrored in the vector containing the Short UTR. These results indicate that although scanning from the cap is inefficient, there is no scanning-independent translation being driven by this UTR in either the bicistronic or the monocistronic hairpin assay.

3.4 The IRES activity of the Long variant and the lack thereof in the Short variant can be observed following direct RNA transfection.

Further experiments were performed on these sequences to definitively show their translational capacities. RNA, functionally similar to messenger RNA, was *in vitro* transcribed. This RNA contains a nucleotide cap and a poly(A) tail. It also contains the UTR of interest, followed by the CAT coding sequence. To control for possible degradation of these synthetic RNAs, each one contains an approximately equal length of UTR sequence. To create transcripts restricted in their capacity for cap-dependent translation, a hairpin sequence was included in the 5' end of each one. Upon transfection of these synthetic transcripts into HEK293 cells, CAT protein and RNA

levels were quantified (Figure 11). The synthetic RNA containing the Long UTR exhibited a 30% drop in translation on hairpin addition (as shown by CAT protein to CAT RNA) ($p< 0.005$). In contrast, the Short UTR RNA showed a significant 90% drop in translation with hairpin inclusion ($p<0.0001$). This data confirms the capacity of the Long UTR to support IRES-dependent translation initiation, while confirming the absence of this ability in the Short UTR. These results also definitively exclude confounding of apparent IRES activity by binding of nuclear proteins or splicing.

3.5 XIAP protein levels increase in serum deprivation and both mRNA isoforms are present in the polyribosomal fractions.

As *ex vivo* characterization has revealed differential activities for the two XIAP UTRs, it was my hypothesis that these mRNA isoforms are responsible for differential regulation of XIAP expression. The role of these transcripts in response to stress will be assessed in a cellular model. Since both XIAP transcripts create an identical protein, an appropriate method had to be designed for use in cells. An RNA Interference approach was developed; efficacy and specificity testing was carried out on monocistronic constructs. As seen in Figure 12, both UTRs could be effectively targeted using siRNA, although the siRNA targeting the Short UTR was consistently better at reducing reporter protein levels. When co-transfected with the construct containing the non-targeted UTR, neither siRNA reduced reporter protein levels, thus confirming specificity of targeting. The effect of each siRNA on endogenous XIAP protein levels was also assessed. XIAP protein levels invariably decreased on treatment with Short UTR-targeting siRNA, but the level of XIAP reduction was variable. Treatment of cells with Long UTR-targeting siRNA did not have any effect on total

Figure 11: The observed translational capacities of the two XIAP UTRs are not artefacts of RNA processing.
(A) Capped and polyadenylated synthetic RNA was transcribed *in vitro*, using a PCR product corresponding to each UTR (and including the CAT coding sequence) as a template. Empty construct as a control. Monocistronic and monocistronic hairpin transcripts were used.
(B) The synthetic RNA were transfected into HEK293 cells in a 12 well plate using Lipofectamine™ 2000, 1μg/well. After 4 hours, cells were lysed for CAT protein determination by ELISA, and CAT RNA quantification using qRT-PCR. A standard curve was used to determine the amount of CAT RNA detected. Results shown as CAT protein normalized to CAT RNA. Data shown is the mean of three biological replicates.

A

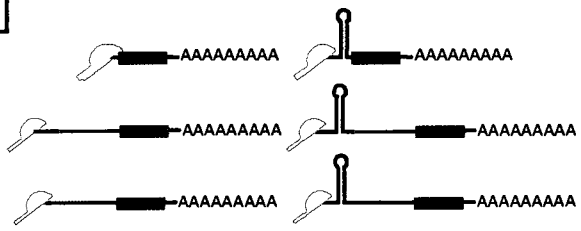
AAAAAAAAA
AAAAAAAAA
AAAAAAAAA
AAAAAAAAA
AAAAAAAAA
AAAAAAAAA

B

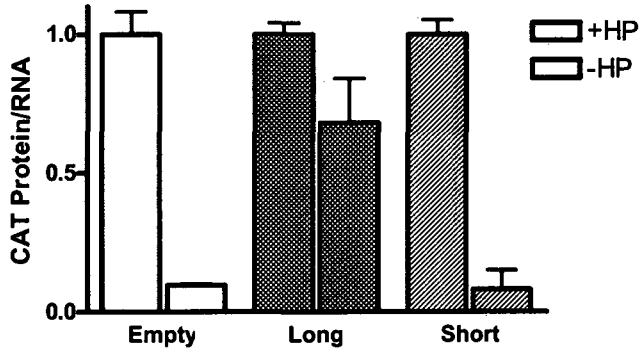
CAT Protein/RNA
1.0
0.5
0.0
Empty
Long
Short
+HP
-HP

Figure 12: An effective and specific RNA Interference approach can be used to target each UTR in reporter constructs; only the Short isoform could be targeted endogenously.

(A) siRNA targeting each transcript was transfected into HEK293 cells in 6 well plates at a concentration of 20 nM, using DharmaFECT™ 1. 24 hours later, 0.5 μg monocistronic construct expressing the corresponding UTR was also transfected into the cells. Cells were lysed after 24 hours, and ELISA methods were used to quantify CAT and Neo protein levels. Results shown as CAT to Neo protein.

(B) Experiment performed as in (A), but transfecting the monocistronic construct containing the opposite UTR with the siRNA. Results shown as CAT to Neo Protein.

(C) HEK293 cells in a 6 well plate were transfected with siRNA (control, Long-targeting, Short-targeting, XIAP coding region-targeting) at a concentration of 20 nM, using DharmaFECT™ 1. After 48 hours, cells were harvested for Western blot analysis. Results quantified using Odyssey densitometry software (Licor) and shown as XIAP to Actin protein.

(D) Transfection as in (C), but RNA was extracted from HEK293 cells and reverse transcription was performed. Quantitative RT-PCR was performed using qXIAP and qActin primers; results obtained through ΔΔct method. Results shown as qXIAP to qActin RNA.

(E) Experiment as in (D), but qPCR was performed using q4496 (Long isoform) and qActin primers; results obtained through ΔΔct method. Results shown as q4496 to qActin RNA.

(F) Experiment as in (D), but qPCR was performed using q323 (Short isoform) and qActin primers; results obtained through ΔΔct method. Results shown as q323 to qActin RNA.

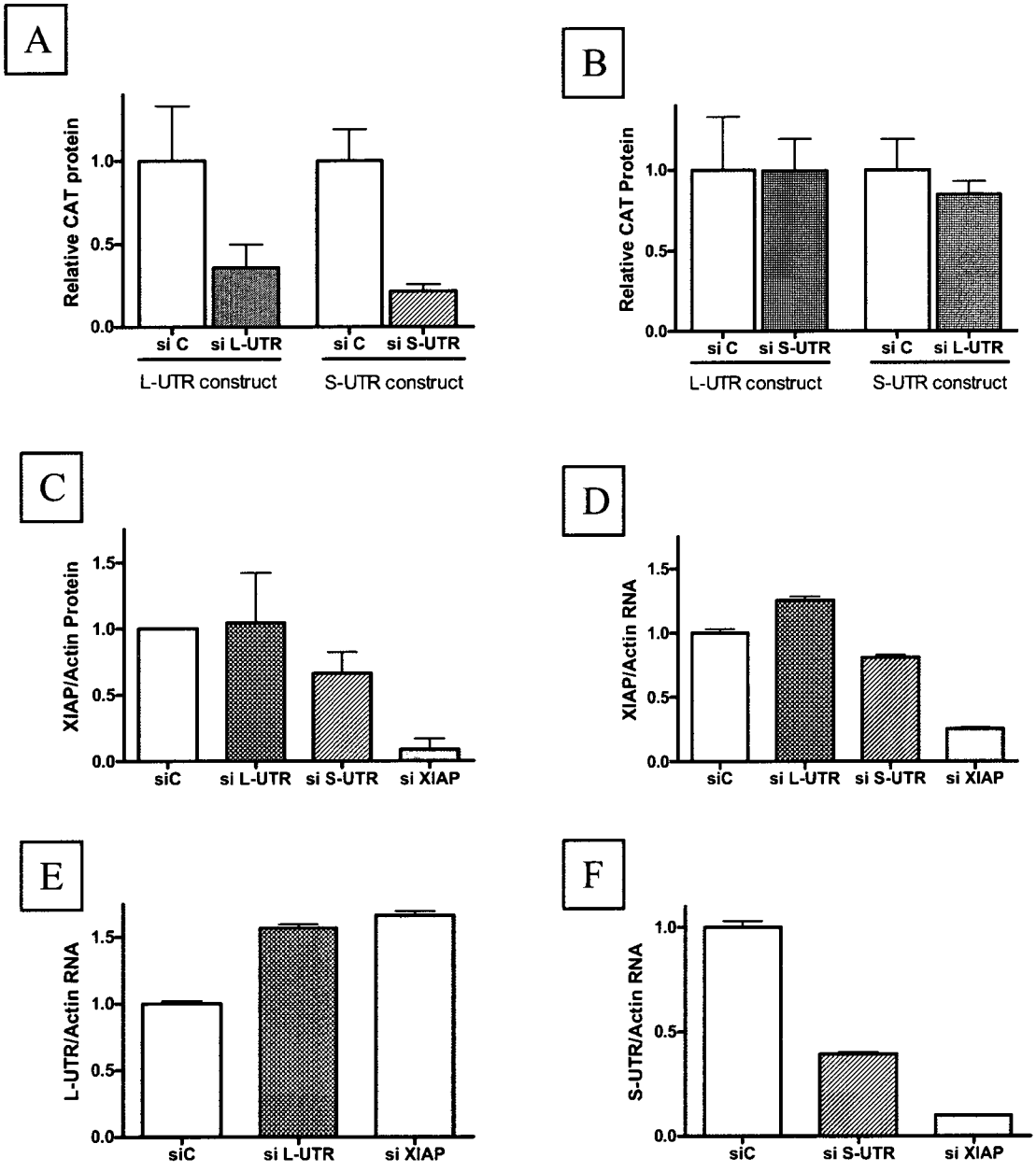
A
Relative CAT protein
1.0
0.5
0.0
si C
si L-UTR
si C
si S-UTR
L-UTR construct
S-UTR construct
B
Relative CAT Protein
1.0
0.5
0.0
si C
si S-UTR
si C
si L-UTR
L-UTR construct
S-UTR construct
C
XIAP/Actin Protein
1.5
1.0
0.5
0.0
siC
si L-UTR
si S-UTR
si XIAP
D
XIAP/Actin RNA
1.5
1.0
0.5
0.0
siC
si L-UTR
si S-UTR
si XIAP
E
L-UTR/Actin RNA
1.5
1.0
0.5
0.0
siC
si L-UTR
si XIAP
F
S-UTR/Actin RNA
1.0
0.5
0.0
siC
si S-UTR
si XIAP

XIAP protein levels. qRT-PCR showed a 60% reduction in Short mRNA levels with RNAi targeted to this sequence, with a corresponding 20% reduction in XIAP coding mRNA (Figure 12). In contrast, no effect on XIAP RNA levels is observed on treatment with siRNA targeting the Long mRNA. The siRNA transfection was effective as evidenced by the depletion of XIAP protein and XIAP mRNA by siRNA targeting the common 3'UTR of XIAP.

As the RNA interference approach was effective in removing the Short isoform, it was used to examine the role of this XIAP transcript in a cellular model of serum starvation. In many cancers, tumours lack a sufficient vascular network. Since they consume nutrients so quickly, the centres of solid tumours often encounter conditions of serum starvation (Folkman, 1976; Thomlinson, and Gray, 1955). In previous work with this model, Holcik *et al.* found that the activity of the XIAP IRES (found in the Long UTR) increases during serum deprivation (Holcik, Lefebvre, et al, 1999). To examine the effect of this treatment on endogenous XIAP, levels of XIAP protein were examined in HEK293 cells following a 48 hr serum starvation. XIAP protein levels consistently increased in these conditions, in parallel with the reported increase in IRES activity (Figure 13A). It was also noted that total levels of XIAP mRNA did not change during serum starvation, so the increase in protein is likely at the translational level. The depletion of phosphorylated ribosomal protein S6 (rpS6) indicates that the serum starvation is having the expected inhibitory effect on the translational machinery (Figure 13B). In an attempt to dissect the XIAP protein response in serum starvation, siRNA targeting the Short mRNA isoform was used. It was found that the increase in XIAP protein in response to serum starvation is maintained following knockdown of the Short mRNA isoform (Figure 13D).

To confirm these observations, the ribosomal recruitment of XIAP mRNA isoforms

Figure 13: XIAP protein production is induced by the Long XIAP mRNA during serum starvation.
(A) HEK293 cells were seeded in a polyD-lysine-coated 6 well plate. Media was removed after 24 hours and after rinsing, either complete DMEM (control) or complete DMEM minus fetal calf serum (starved) was added to the well. Cells were harvested for Western blot analysis after 48 hours. Results quantified using Odyssey densitometry software (Licor) and shown as XIAP to Actin protein. Statistical significance determined by unpaired T test (*, $p<0.05$)
(B) Representative Western blot image. Phosphorylation status of rpS6 to ensure starvation is affecting translation in cells.
(C) Experiment as in (A), but RNA extracted from HEK293 cells and reverse transcription was performed. Quantitative RT-PCR was performed using qXIAP and qActin primers; results obtained through $\Delta\Delta$ct method. Results shown as qXIAP to qActin RNA.
(D) Experiment as in (A), but 24 hours after seeding, 20nM siRNA specific to the Short isoform sequence or scrambled control siRNA (siC) was added to the well. 24 hours later, serum starvation as in (A). Cells were harvested for Western blot analysis after 48 hours. Results quantified using Odyssey densitometry software (Licor) and shown as XIAP to Actin protein. Control (complete DMEM) set to 1. Statistical significance found using unpaired T tests (*, $p<0.05$)
(E) Representative Western blot image.

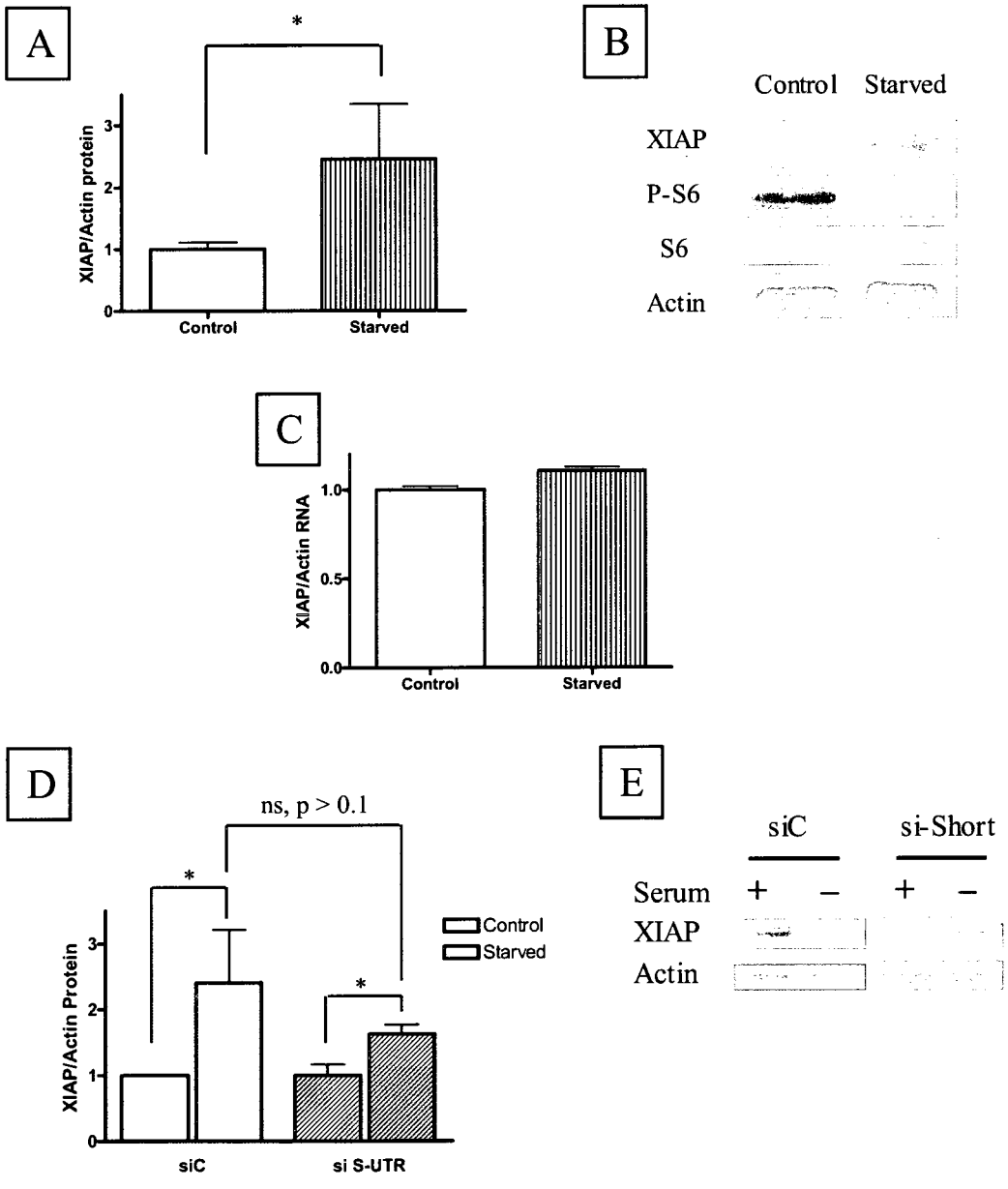
A
*
XIAP/Actin protein
3
2
1
0
Control
Starved
B
Control
Starved
XIAP
P-S6
S6
Actin
C
XIAP/Actin RNA
1.0
0.5
0.0
Control
Starved
D
ns, p > 0.1
*
*
XIAP/Actin Protein
3
2
1
0
Control
Starved
siC
si S-UTR
E
siC
si-Short
Serum
+
–
+
–
XIAP
Actin

was investigated during serum starvation using a polysome profiling technique (Figure 14). Following 24 hours of serum deprivation, RNA was extracted and loaded onto a sucrose gradient. Separation of the ribosome-bound transcripts was achieved through ultracentrifugation, and the monosomal and polysomal fractions were collected. Semi-quantitative PCR was used to determine the RNA levels in each fraction. Transcripts found in the heavier fractions are associated with many ribosomes, indicating a high level of translation. Transcripts found in the low polysomal and monosomal fractions are not being highly translated. Serum starvation had the expected effect on the mRNA coding for the housekeeping protein GAPDH, decreasing its level of ribosomal recruitment and shifting it to the light polysomal fraction. Surprisingly, both XIAP transcripts maintained their polyribosomal distribution under serum deprivation conditions.

3.6 XIAP protein levels are maintained in rapamycin treatment and both XIAP variants are found in the polyribosomal fractions.

To examine translation of the two XIAP mRNA isoforms in another cellular stress model, the drug rapamycin was used to inhibit cap-dependent translation. Rapamycin has many effects on the cell, including a suppressive effect on translation. This effect is mediated by the inhibition of mTOR (mammalian target of rapamycin) signalling, as well as the dephosphorylation of 4E-BPs, resulting in the sequestration of eIF4E (Beretta, Gingras, et al, 1996; Chen, Yang, et al, 2009; Dumont, and Su, 1996). As eIF4E plays a significant role in cap-dependent translation, rapamycin causes a decrease in global translation levels. The effect of rapamycin treatment on translation of each transcript was examined in HPV-transformed human keratinocytes (HF1-E cells) obtained from Dr. Alexander Levitzki (Mizrachy-Schwartz, Kravchenko-Balasha,

Figure 14: Both XIAP mRNA isoforms are found in the high polyribosomal fraction during serum starvation.
(A) To examine ribosomal recruitment of each transcript, cycloheximide-fixed RNA was sedimented through a sucrose gradient using ultracentrifugation. The profile of the RNA (as indicated by absorbance at 254 nm) is shown for HEK293 cells under normal growth conditions (Control) as well as following 24 hours of serum starvation (Starved).
(B) Ribosomal recruitment of XIAP mRNA isoforms under control and starved conditions. Semi-quantitative RT-PCR was performed on an equal volume of each fraction (fractions spiked with CAT RNA prior to processing, to ensure technical consistency in fraction handling). Results quantified using Odyssey densitometry software (Licor). Electrophoretic analysis of raw semi-quantitative PCR shown. Results shown as a percentage of the total Long or Short XIAP mRNA found in all fractions.
(C) Ribosomal recruitment of GAPDH RNA, as in (B). Results shown as percentage of total GAPDH RNA found in all fractions.

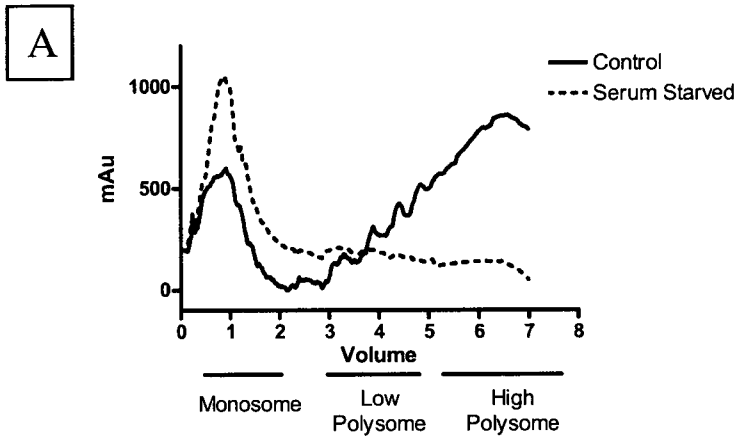
A
Control
Serum Starved
1000
500
0
mAu
0 1 2 3 4 5 6 7 8
Volume
Monosome
Low Polysome
High Polysome

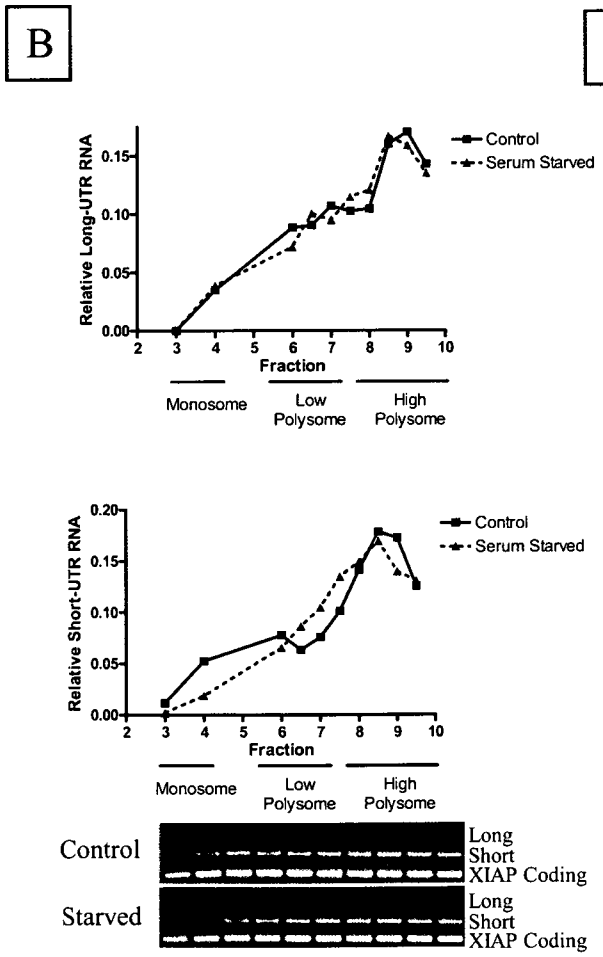
B
Relative Long-UTR RNA
0.15
0.10
0.05
0.00
2 3 4 5 6 7 8 9 10
Fraction
Control
Serum Starved
Monosome
Low Polysome
High Polysome
Relative Short-UTR RNA
0.20
0.15
0.10
0.05
0.00
2 3 4 5 6 7 8 9 10
Fraction
Control
Serum Starved
Monosome
Low Polysome
High Polysome
Control
Long
Short
XIAP Coding
Starved
Long
Short
XIAP Coding

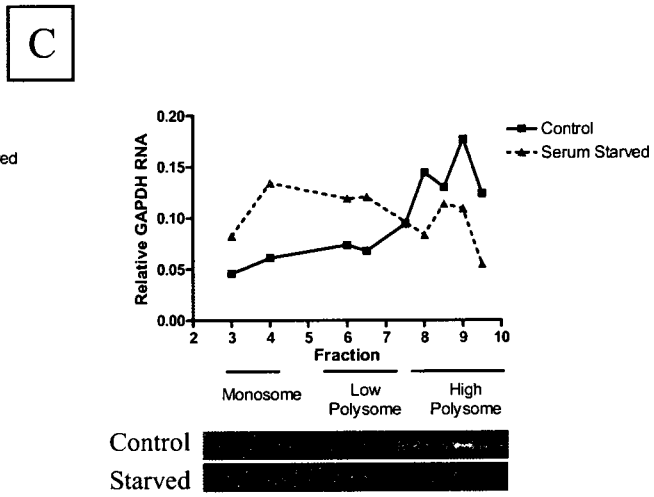
C
Relative GAPDH RNA
0.20
0.15
0.10
0.05
0.00
2 3 4 5 6 7 8 9 10
Fraction
Control
Serum Starved
Monosome
Low Polysome
High Polysome
Control
Starved

et al, 2007). The HF1-E cells were treated with 150nM rapamycin for 24 hrs, and total XIAP protein levels, as well as the translation of each transcript, were examined using Western blotting and polysomal profiling. Total XIAP protein levels are maintained on rapamycin treatment, whereas levels of Actin protein decreased (Figure 15). Ribosomal recruitment of the XIAP mRNA isoforms was next explored, through determination of the their distribution within a polysomal gradient. When contrasted to EEF1A1 and GAPDH, which clearly shifts out of the heavy polysomal fraction, both XIAP mRNA isoforms are maintained in the polysome following rapamycin treatment (Figure 16).

Figure 15: XIAP protein levels are maintained during rapamycin treatment
(A) HF1-E cells were seeded 1:2 in 6 well plates in KGM. After 24 hours, media was replaced with KGM containing DMSO or 150 nM Rapamycin. Cells were harvested after 24 hours for Western blot analysis. Results quantified using Odyssey densitometry software (Licor) and shown as XIAP to Actin protein.
(B) Representative Western blots used for quantitation in (A) and confirmation of rapamycin efficacy (dephosphorylation of rpS6).

A

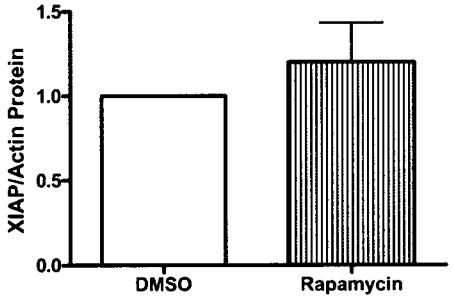
1.5
1.0
0.5
0.0
XIAP/Actin Protein
DMSO
Rapamycin

B

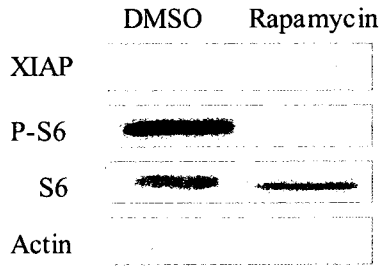
DMSO
Rapamycin
XIAP
P-S6
S6
Actin

Figure 16: Both XIAP mRNA isoforms are found in the high polyribosomal fraction during rapamycin treatment

(A) To examine ribosomal recruitment of each transcript, cycloheximide-fixed RNA was sedimented through a sucrose gradient using ultracentrifugation. The profile of the RNA (as indicated by absorbance at 254 nm) is shown for HF1-E cells under normal growth conditions (Control) as well as following 24 hours of rapamycin treatment (Rapamycin). Rapamycin experiment only performed once.

(B) Ribosomal recruitment of XIAP mRNA isoforms under control and rapamycin treatment. Semi-quantitative RT-PCR was performed on an equal volume of each fraction (fractions spiked with CAT RNA prior to processing, to ensure technical consistency in fraction handling). Results quantified using Odyssey densitometry software (Licor). Electrophoretic analysis of raw semi-quantitative PCR shown. Results shown as a percentage of the total Long or Short XIAP mRNA found in all fractions.

(C) Ribosomal recruitment of GAPDH RNA, as in (B). Results shown as percentage of total GAPDH RNA found in all fractions.

(D) Ribosomal recruitment of EEF1A1 RNA, as in (B). Results shown as percentage of total EEF1A1 RNA found in all fractions.

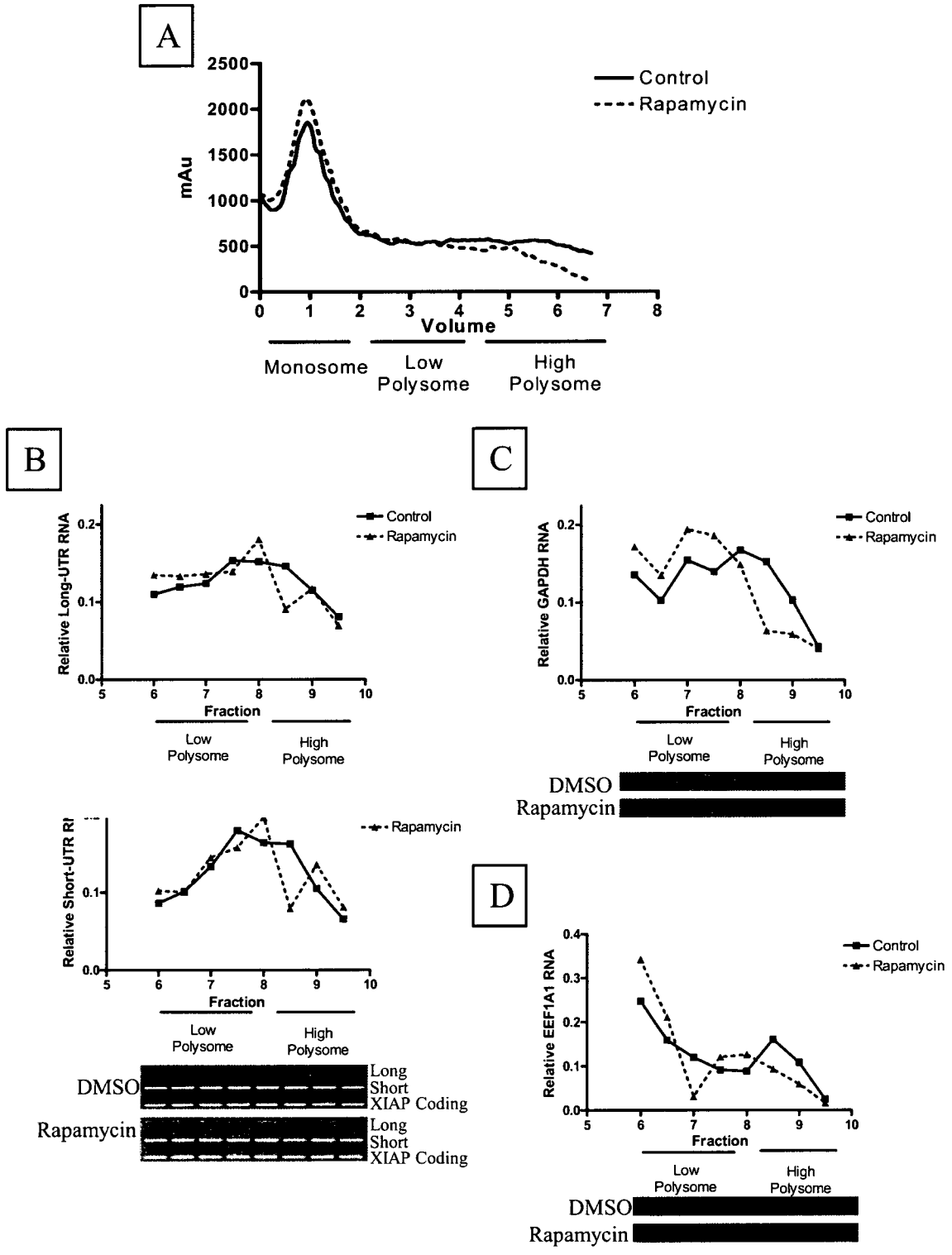
A
2500
2000
1500
1000
500
0
mAu
0 1 2 3 4 5 6 7 8
Volume
Control
Rapamycin
Monosome
Low Polysome
High Polysome
B
Relative Long-UTR RNA
0.2
0.1
0.0
5 6 7 8 9 10
Fraction
Control
Rapamycin
Low Polysome
High Polysome
Relative Short-UTR RI
Rapamycin
DMSO
Rapamycin
Long
Short
XIAP Coding
C
Relative GAPDH RNA
Control
Rapamycin
Fraction
Low Polysome
High Polysome
DMSO
Rapamycin
D
Relative EEF1A1 RNA
0.4
0.3
0.2
0.1
0.0
Control
Rapamycin
Fraction
Low Polysome
High Polysome
DMSO
Rapamycin

Chapter 4: Discussion

During cellular stress conditions, the intrinsic caspase inhibitor XIAP plays a critical role in the delay or even prevention of apoptosis. The layers of control evident in XIAP expression and activity highlight the importance of the XIAP protein. The previously described 5'UTR of XIAP has been shown to contain a strong, biologically relevant internal ribosome entry site (IRES) (Gu, Zhu, et al, 2009; Holcik, Lefebvre, et al, 1999; Holcik, Yeh, et al, 2000; Holcik, and Korneluk, 2000; Holcik, 2003; Holcik, Graber, et al, 2005; Spahn, Blondeau, et al, 2008; Yoon, Peng, et al, 2006). The XIAP IRES is essential to the increase in cellular XIAP levels under stress situations (Gu, Zhu, et al, 2009; Holcik, Lefebvre, et al, 1999; Holcik, Yeh, et al, 2000; Nevins, Harder, et al, 2003; Yoon, Peng, et al, 2006). A second mRNA isoform also coding for the XIAP protein has been identified in the EST database (Gu, Zhu, et al, 2009; Van Eden, Byrd, et al, 2004a) although its relevance to XIAP expression remains unclear. These mRNA isoforms contain distinct 5'UTR sequences, although their coding regions and 3'UTRs are identical. The variants could arise from two different promoters, or as a result of alternative splicing. This research focuses on XIAP regulation at the level of translational control, through these alternate transcripts. Specifically, the two variants of the XIAP transcript were characterized, and their biological roles examined.

I have shown here that both mRNA isoforms were found in a diverse panel of tumour and transformed cell lines. The Long XIAP mRNA isoform was consistently present at lower levels than the Short isoform in these cell lines. This finding may represent the endogenous situation, or it could be a result of technical difficulties. To rule out technical problems of my approach, I tested the primers on DNA constructs and the reverse transcription reaction on *in vitro*-synthesized RNA. The PCR and the reverse

transcription were found to be equally efficient for both isoform sequences, indicating that the difference in abundance is biological, and reflects the true abundance of each XIAP isoform in the cell. This difference could result from a number of reasons; transcription of the Short isoform could be occurring more often or degradation of the Long isoform could be occurring more quickly. Another possibility is that if these isoforms are a result of alternative splicing, production of the Short isoform could be favoured. Since the Long isoform has been shown previously to be important in transient stress (Holcik, Lefebvre, et al, 1999; Holcik, Yeh, et al, 2000), and instability is a hallmark of mRNA coding for transiently required proteins, it is possible that these differences in abundance result from increased mRNA instability, and thus accelerated degradation of the Long isoform.

Examination of each 5'UTR revealed differential translational capacities for each. The Long UTR was found to have no effect on expression of a downstream cistron in a cap-dependent context, and the presence of a *bona fide* IRES in the Long UTR was confirmed. In contrast, the Short UTR was found to have an inhibitory effect on cap-dependent translation of a downstream cistron. I have also shown that there is no IRES-dependent translational activity enabled by the Short UTR.

The translational capacities of each transcript were examined using three distinct approaches: a bicistronic assay, a monocistronic hairpin assay, and a synthetic RNA assay. Although much research has been dedicated to the Long XIAP mRNA (reviewed in Lewis, and Holcik, 2005), the validity of the bicistronic assay used to test its IRES activity has been recently questioned (Kozak, 2001; Van Eden, Byrd, et al, 2004a). There is no consensus sequence or structure that can be used to identify cellular IRESes, therefore all IRESes must be empirically tested (Baird, Turcotte, et al, 2006). A bicistronic reporter assay is considered the gold standard in the field of IRES research,

and has been widely used (Mokrejs, Vopalensky, et al, 2006; Sachs, 2000). However, the widely used firefly/renilla luciferase variant of this assay has been found to be flawed, ascribing protein production resulting from spurious splicing to several putative IRES elements, including XIAP (Van Eden, Byrd, et al, 2004a). Although these errors were not observed in the βgal/CAT construct used to initially characterize the XIAP IRES, some controversy remains (Baranick, Lemp, et al, 2008; Holcik, Graber, et al, 2005). It has been suggested that in order to definitively characterize a putative IRES element, stringent testing methods must be used (Kozak, 2001; Van Eden, Byrd, et al, 2004b). The research described here made use of numerous rigorous methods to assess the translational capacities of each XIAP mRNA variant.

Using these approaches, the activity of the IRES element present in the Long UTR was confirmed. This IRES element elevated cap-independent translation of the second cistron in the bicistronic reporter RNA by more than 50-fold. It has also been shown here that translation of the Long UTR of XIAP is almost exclusively IRES driven. This could be observed in the hairpin construct experiments, when blocking scanning from the cap had no effect on the amount of protein produced, when compared to the hairpin-less construct. This indicates that although there is not a negative effect on translation of a downstream cistron, it is because the IRES element translates at high enough efficiency to replace the blocked cap-dependent translation. The inability of the Long UTR to allow cap-dependent translation is most likely a result of numerous upstream start codons and projected RNA structure, which can have an inhibitory effect on ribosome scanning (reviewed in Babendure, Babendure, et al, 2006; Iacono, Mignone, and Pesole, 2005; Pickering, and Willis, 2005). The Long UTR is also much longer than the average 5'UTR (~150nt), which could play a role in the inhibition of scanning (Baird, Turcotte, et al, 2006).

The maintenance of IRES-mediated translation of the Long UTR in the synthetic RNA experiment clearly shows the ability of this UTR to drive translation initiation, even in the absence of the *in vivo* process of transcription. As transcription can often be closely associated with splicing and the binding of nuclear proteins, direct RNA transfection excludes these events from being responsible for the observed IRES activity in the Long isoform. However, despite the efficient translation driven by this UTR, this isoform is unlikely to contribute much XIAP protein to the cellular XIAP pool under normal growth conditions, due to its low abundance.

The Short XIAP mRNA isoform differs from the Long variant in terms of translational capacity. As shown in the bicistronic, monocistronic and synthetic RNA experiments, this UTR is not capable of driving IRES-mediated translation, and relies on ribosome scanning from the cap. This isoform also represses translation of a downstream cistron by more than 50%. Due to the high G/C content in the Short 5'UTR, a significant amount of secondary structure would be expected. Since mRNA structure has been demonstrated to have an inhibitory effect on ribosomal scanning from the cap, this could explain the decrease in protein produced from a downstream cistron (Dever, 2002; Kozak, 1989a).

The characterization of the 5'UTR of each mRNA variant led to an interesting hypothesis. As these two isoforms appear to utilise exclusive mechanisms of translation, it is likely that they are differently important in the cell. As both isoforms code for an identical XIAP protein, it was necessary to develop an approach that could separate the actions of each mRNA isoform. RNA interference makes use of short interfering RNA (siRNA) oligonucleotides complementary to part of a targeted mRNA (usually the 3'UTR). Upon binding to the targeted sequence, RNA degradation proteins are recruited, and a specific knockdown of the target mRNA occurs (Hannon, 2002). An RNA

interference approach was developed to characterize the role of the XIAP mRNA isoforms in a cellular model. The siRNAs were designed such that they targeted the distinct 5'UTRs of the isoforms, and efficacy and specificity testing were done on transfected constructs containing one or the other UTR. Development of this technique was fraught with difficulties. The constructs containing the Short UTR could be efficiently targeted using a pool of the first two siRNAs attempted. As for the Long UTR, three different Long-UTR targeting siRNAs from Invitrogen, as well as three from Qiagen, were tested. An endoribonuclease-prepared siRNA approach was also tried (Yang, Buchholz, et al, 2002). One of the three from Qiagen was able to specifically decrease levels of the Long-UTR containing construct, and was subsequently tested on endogenous XIAP mRNA.

Although siRNA could clearly reduce levels of a reporter mRNA and protein containing the Long UTR, endogenous XIAP protein and RNA were not reduced in a cellular model. This could be due to the low levels of this XIAP isoform, or to the inaccessibility of siRNA targeting sites in the context of full length mRNA. As I do see an increase in XIAP mRNA upon treatment with siRNA to the Long isoform, it is also possible that the siRNA are targeting a possible promoter region, a situation which has been found to activate transcription of specific mRNAs (Li,L.C. 2006; Janowski, Younger, et al, 2007).

In contrast, the siRNA-mediated targeting of the Short mRNA isoform resulted in approximately 20% reduction in XIAP coding RNA. When the levels of Short isoform mRNA were examined, it was found that there is more than a 50% reduction by the siRNA. The siRNA results in a ~30% lowering in total XIAP protein levels, and since it is only ~50% effective at targeting the Short mRNA isoform, the results suggest that this XIAP isoform contributes to at least 60% of the endogenous XIAP protein. It appears that the high abundance of this mRNA isoform allows it to overcome its translational

impediments to become a major contributor to basal XIAP protein levels. The XIAP protein remaining following siRNA-mediated knockdown is likely being contributed by the Long mRNA isoform. Although it would have been ideal if the RNA interference approach could have been optimized for both XIAP mRNA variants, the efficacy of the siRNA targeting the Short isoform enabled indirect characterization of each mRNA in a model of cellular stress.

Once the siRNA approach had been optimized for the Short isoform, I began to search for a model of cellular stress in which I could examine the behaviour of these two XIAP mRNA variants. Previous studies have identified serum starvation as a biologically relevant stress condition that can be used to observe differential mRNA activities (Nevins, Harder, et al, 2003). During serum starvation, global protein synthesis is attenuated, through phosphorylation of eIF2α and cleavage of eIF4G (Clemens, Bushell, et al, 2000). The translation of mRNAs that code for proteins important to the stress response is maintained, or even increased (Holcik, Sonenberg, and Korneluk, 2000).

Previous studies have identified that the activity of the XIAP IRES increases under conditions of serum starvation (Holcik, Lefebvre, et al, 1999). This correlates well with XIAP's anti-apoptotic role in cellular stress. The serum starvation model was thus chosen to test the activities of the XIAP mRNA isoforms under cellular stress conditions.

To find the effect of serum starvation on XIAP protein levels, HEK293 cells were grown in serum-free media for 24 hours and protein levels were examined by western blotting. Following starvation, XIAP levels rose considerably in comparison to a housekeeping protein, although RNA levels were unchanged, indicating a translational component to the XIAP protein upregulation.

To examine the roles of the mRNA variants under conditions of serum deprivation, HEK293 cells that had been growing in normal media were transfected with either non-targeting control siRNA or siRNA to deplete the Short isoform. The increase in XIAP protein following serum deprivation was observed in cells transfected with both the control siRNA and Short UTR-siRNA. The difference between the increase in Short-UTR siRNA-treated cells and the one observed after treatment with control siRNA is not significant as determined by an unpaired t-test. The observed results imply that the Long isoform is responsible for the increase in protein, and although the removal of the Short isoform reduces total XIAP levels, it does not affect the starvation-induced increase. An alternative explanation is that the increase in XIAP protein is due to the activity of a previously uncharacterized additional transcript. This is less likely, as the importance of the XIAP IRES element in stress conditions has been well documented (Gu, Zhu, et al, 2009; Holcik, Lefebvre, et al, 1999; Holcik, Yeh, et al, 2000; Nevins, Harder, et al, 2003; Yoon, Peng, et al, 2006). As RNA interference was ineffective for the Long XIAP variant, the direct roles of this isoform in XIAP protein upregulation in this model could not be definitively elucidated.

The translational capacities of the mRNA variants were then examined under serum starvation conditions, using polysomal profiling. This technique relies on the separation of transcripts according to the amount of ribosomes they are associated with. Highly translated mRNAs will be associated with many ribosomes, and will therefore be present in the high polyribosomal fractions.

Polysomal fractionation was used to assess the translation of both XIAP mRNA isoforms under cellular stress conditions, when global translation is restricted. The presence of the Long mRNA isoform in the high polyribosomal fraction in serum starved cells suggests that this mRNA is still being efficiently translated, even when other mRNAs, such as the

GAPDH mRNA, are not. This fits well with the fact that XIAP is critical in the response to cellular stress (Bratton, Lewis, et al, 2002; Chawla-Sarkar, Bae, et al, 2004; Emamaullee, Rajotte, et al, 2005; Gottfried, Rotem, et al, 2004; Holcik, Lefebvre, et al, 1999; Holcik, Yeh, et al, 2000; Karikari, Roy, et al, 2007; Spahn, Blondeau, et al, 2008).

Interestingly, the Short XIAP mRNA isoform is also retained in the polyribosomal fraction following serum starvation, despite the block in general translation. This would indicate that despite its lack of IRES activity, this transcript is still capable of ribosomal recruitment under starvation conditions. This XIAP isoform may belong to a subset of mRNA that rely on cap-dependent translation initiation, yet alternative mechanisms such as ribosomal shunting allow efficient translation in stress (Jackson, 2005; Tesfay, Yin, et al, 2008). However, as seen in the siRNA experiment, this transcript is not responsible for the increased level of XIAP protein under stress. It is possible that there is an alternate explanation for the retention of the Short isoform in the polyribosomal fraction. A recent study has shown that mRNA found in complexes similar to polyribosomes (pseudo-polysomes) is actually translationally repressed (Thermann, and Hentze, 2007). If this mechanism is occurring here, it could provide an alternate explanation for the ribosomal recruitment of the Short mRNA isoform.

To further examine the activity of the XIAP mRNA isoforms in cellular stress conditions, an alternate model was sought. The drug rapamycin was chosen to impair global translation in a cellular model. This model has been used previously to find differences in translation in two 5'UTR-variants of the ELK-1 mRNA (Araud, Genolet, et al, 2007). Rapamycin is a multi-functional macrolide used for immunosuppression and cancer treatment (Bjornsti, and Houghton, 2004; Grunwald, DeGraffenried, et al, 2002; Neshat, Mellinghoff, et al, 2001; Podsypanina, Lee, et al, 2001; Sehgal, 1998; Shi, Frankel, et al, 1995). It restricts cell growth and proliferation through signalling pathways that affect

protein synthesis. Rapamycin binds mTOR (mammalian target of rapamycin), which inhibits the activation of downstream signalling molecules in the mTOR pathway, imposing a translational slowdown and concordant decrease in total protein synthesis (Abraham, 2002; Schmelzle, and Hall, 2000; Shamji, Nghiem, and Schreiber, 2003). Rapamycin also causes a more specific inhibition of the cap-dependent translational pathway through stimulation of 4E-BP dephosphorylation (Beretta, Gingras, et al, 1996). Hypophosphorylated 4E-BPs have a high affinity for the eIF4G-binding site of eIF4E; 4E-BP binding essentially sequesters eIF4E from participation in the mRNA cap recruitment step of translation. This specifically impedes cap-dependent translation initiation.

A recent study using rapamycin to attenuate cap-dependent protein synthesis in HPV-transformed human keratinocytes described an interesting set of results that could be explained by the presence of two XIAP transcripts (Mizrachy-Schwartz, Kravchenko-Balasha, et al, 2007). In this model, XIAP protein levels were rapamycin-sensitive in primary cells, but rapamycin-resistant in transformed cells. My model would predict that this could be the result of primary cells deriving XIAP mainly from the Short isoform, while the transformed cells depend on the Long variant for XIAP production.

To investigate rapamycin resistance of XIAP protein in the context of two XIAP mRNA isoforms, transformed HF1-E cells were treated with rapamycin for 24 hours, followed by examination of protein levels and translational profiling. XIAP protein levels were maintained following rapamycin treatment. Surprisingly, both XIAP mRNAs were able to escape the rapamycin-imposed inhibition on translation initiation. The maintenance of translation of the Long mRNA under rapamycin treatment was expected, due to its well-characterized IRES element. Unexpectedly, the Short variant was also retained in the high polyribosomal fraction following rapamycin treatment. It has been shown

previously that rapamycin has the strongest effect on a subset of capped mRNAs containing a 5'TOP (terminal oligopyrimidine tract), while having a less profound effect on global translation (Anand, and Gruppuso, 2006; Hamilton, Stoneley, et al, 2006; Jefferies, Reinhard, et al, 1994). This may help to explain the observed retention of the Short mRNA isoform in the high polysomal fraction. Alternatively, the Short variant may be capable of an alternative form of translation, such as the ribosome shunting described earlier. It is also possible that if the Short mRNA isoform is indeed repressed in microRNA-mediated pseudo-polysomes during serum starvation, it correlates that this mechanism would be observed in the rapamycin model as well. It is possible that during the process of transformation, the roles of the mRNA isoforms have evolved, and a different trend may be observed in non-transformed cells.

Previous studies of the XIAP protein under conditions where cap-dependent translation is attenuated with rapamycin have been conflicted. The presence of two XIAP transcripts may help to explain this discrepancy. In some cell line models, treatment with rapamycin causes an increase in XIAP protein levels (Desplanques, Giuliani, et al, 2009), where in others, XIAP expression decreases on treatment (Yan, Frost, et al, 2006). The increase observed in some models has been attributed to XIAP IRES activity, but it is unclear why this increase is not always observed. With the knowledge that there are two XIAP mRNA isoforms, with different possible regulations, it could be that in the cell lines for which XIAP levels did not increase on rapamycin, the XIAP being expressed is due to Short UTR transcript. As this transcript is not capable of cap-independent translation initiation, it could explain why XIAP does not increase in these cell lines.

Through these two cellular models, I have begun to explore the roles of the alternative XIAP mRNA isoforms in cellular stress. The translational activity of these variants was

characterized in both conditions, and their differential effects on XIAP protein production were examined in the serum starvation model.

The mechanism of tight protein regulation through the presence of alternate non-coding regions has been described previously (reviewed in Hughes, 2006). The presence of alternate regulatory regions in mRNAs coding for the same protein allows an additional level of control in terms of location and timing of protein expression. These untranslated regions can effect changes on protein levels in a number of ways, including differences in mRNA stability, translational activity, or differential recruitment of cellular proteins (Al-Fageeh, and Smales, 2009; Wang, Guo, et al, 2009; Zhao, Chen, et al, 2009).

Many proteins expressed through an IRES element are also subject to regulation by alternate non-coding regions (Martineau, Le Bec, et al, 2004; Pozner, Goldenberg, et al, 2000). The angiogenic factor FGF-1 is regulated in this fashion. There are four mRNA isoforms coding for FGF-1; only two isoforms are capable of driving high amounts of IRES-mediated translation initiation (Martineau, Le Bec, et al, 2004). Another example of this type of complex translational regulation is seen in the expression of the neurotrophin receptor TrkB, which is regulated by both IRES activity and the presence of alternate transcripts (Dobson, Minic, et al, 2005). The data shown here suggest that this combination of alternate regulatory regions and IRES activity mediate regulation of XIAP expression as well.

In summary, the two XIAP mRNA isoforms have been demonstrated to have distinct modes of operation, implying a tight regulation of XIAP protein production through differential actions under cellular stress. Their distinct mechanisms of action have been delineated here and tested in two different models, with each variant shown to contribute to XIAP protein under distinct conditions.

Conclusion

From the experiments detailed in this document, it is clear that XIAP expression is highly regulated at the level of translation initiation. The internal ribosome entry site in the Long XIAP mRNA isoform has been confirmed, and the lack of such an element in the Short variant has been described. The Long isoform is translated solely through its IRES, while the Short isoform is expressed in a completely cap-dependent fashion. The Short mRNA isoform does have a repressive effect on translation, but due to the comparatively high endogenous presence of this isoform, it is responsible for maintaining XIAP protein levels under normal growth conditions. The Long mRNA variant plays a role in the XIAP protein response to serum starvation and both transcripts are associated with polyribosomes during serum starvation and rapamycin treatment. The characterization of these transcripts opens the way to research that may enable using these alternate isoforms as therapeutic targets in cell death diseases and carcinomas, where XIAP plays a critical role.

References

Abbott, C.M., and Proud, C.G. (2004). Translation factors: in sickness and in health. Trends Biochem. Sci. *29,* 25-31.

Abraham, R.T. (2002). Identification of TOR signaling complexes: more TORC for the cell growth engine. Cell *111,* 9-12.

Acehan, D., Jiang, X., Morgan, D.G., Heuser, J.E., Wang, X., and Akey, C.W. (2002). Three-dimensional structure of the apoptosome: implications for assembly, procaspase-9 binding, and activation. Mol. Cell *9,* 423-432.

Al-Fageeh, M.B., and Smales, C.M. (2009). Cold-inducible RNA binding protein (CIRP) expression is modulated by alternative mRNAs. RNA *15,* 1164-76

Anand, P., and Gruppuso, P.A. (2006). Rapamycin inhibits liver growth during refeeding in rats via control of ribosomal protein translation but not cap-dependent translation initiation. J. Nutr. *136,* 27-33.

Araud, T., Genolet, R., Jaquier-Gubler, P., and Curran, J. (2007). Alternatively spliced isoforms of the human elk-1 mRNA within the 5' UTR: implications for ELK-1 expression. Nucleic Acids Res. *35,* 4649-4663.

Babendure, J.R., Babendure, J.L., Ding, J.H., and Tsien, R.Y. (2006). Control of mammalian translation by mRNA structure near caps. RNA *12,* 851-861.

Baird, S.D., Lewis, S.M., Turcotte, M., and Holcik, M. (2007). A search for structurally similar cellular internal ribosome entry sites. Nucleic Acids Res. *35,* 4664-4677.

Baird, S.D., Turcotte, M., Korneluk, R.G., and Holcik, M. (2006). Searching for IRES. RNA *12,* 1755-1785.

Baranick, B.T., Lemp, N.A., Nagashima, J., Hiraoka, K., Kasahara, N., and Logg, C.R. (2008). Splicing mediates the activity of four putative cellular internal ribosome entry sites. Proc. Natl. Acad. Sci. U. S. A. *105,* 4733-4738.

Beretta, L., Gingras, A.C., Svitkin, Y.V., Hall, M.N., and Sonenberg, N. (1996). Rapamycin blocks the phosphorylation of 4E-BP1 and inhibits cap-dependent initiation of translation. EMBO J. *15,* 658-664.

Bjornsti, M.A., and Houghton, P.J. (2004). The TOR pathway: a target for cancer therapy. Nat. Rev. Cancer. *4,* 335-348.

Boldin, M.P., Goncharov, T.M., Goltsev, Y.V., and Wallach, D. (1996). Involvement of MACH, a novel MORT1/FADD-interacting protease, in Fas/APO-1- and TNF receptor-induced cell death. Cell *85,* 803-815.

Bratton, S.B., Lewis, J., Butterworth, M., Duckett, C.S., and Cohen, G.M. (2002). XIAP inhibition of caspase-3 preserves its association with the Apaf-1 apoptosome and prevents CD95- and Bax-induced apoptosis. Cell Death Differ. *9,* 881-892.

Braunstein, S., Karpisheva, K., Pola, C., Goldberg, J., Hochman, T., Yee, H., Cangiarella, J., Arju, R., Formenti, S.C., and Schneider, R.J. (2007). A hypoxia-controlled cap-dependent to cap-independent translation switch in breast cancer. Mol. Cell *28,* 501-512.

Chai, J., Shiozaki, E., Srinivasula, S.M., Wu, Q., Datta, P., Alnemri, E.S., and Shi, Y. (2001). Structural basis of caspase-7 inhibition by XIAP. Cell *104,* 769-780.

Chawla-Sarkar, M., Bae, S.I., Reu, F.J., Jacobs, B.S., Lindner, D.J., and Borden, E.C. (2004). Downregulation of Bcl-2, FLIP or IAPs (XIAP and survivin) by siRNAs sensitizes resistant melanoma cells to Apo2L/TRAIL-induced apoptosis. Cell Death Differ. *11,* 915-923.

Chen, R.Q., Yang, Q.K., Lu, B.W., Yi, W., Cantin, G., Chen, Y.L., Fearns, C., Yates, J.R.,3rd, and Lee, J.D. (2009). CDC25B mediates rapamycin-induced oncogenic responses in cancer cells. Cancer Res. *69,* 2663-2668.

Clemens, M.J. (1994). Regulation of eukaryotic protein synthesis by protein kinases that phosphorylate initiation factor eIF-2. Mol. Biol. Rep. *19,* 201-210.

Clemens, M.J., Bushell, M., Jeffrey, I.W., Pain, V.M., and Morley, S.J. (2000). Translation initiation factor modifications and the regulation of protein synthesis in apoptotic cells. Cell Death Differ. *7,* 603-615.

Clemens, M.J., Bushell, M., and Morley, S.J. (1998). Degradation of eukaryotic polypeptide chain initiation factor (eIF) 4G in response to induction of apoptosis in human lymphoma cell lines. Oncogene *17,* 2921-2931.

Cornelis, S., Tinton, S.A., Schepens, B., Bruynooghe, Y., and Beyaert, R. (2005). UNR translation can be driven by an IRES element that is negatively regulated by polypyrimidine tract binding protein. Nucleic Acids Res. *33,* 3095-3108.

Crook, N.E., Clem, R.J., and Miller, L.K. (1993). An apoptosis-inhibiting baculovirus gene with a zinc finger-like motif. J. Virol. *67,* 2168-2174.

Cryns, V., and Yuan, J. (1998). Proteases to die for. Genes Dev. *12,* 1551-1570.

Dean, E., Jodrell, D., Connolly, K., Danson, S., Jolivet, J., Durkin, J., Morris, S., Jowle, D., Ward, T., Cummings, J. *et al.* (2009). Phase I trial of AEG35156 administered as a 7-day and 3-day continuous intravenous infusion in patients with advanced refractory cancer. J. Clin. Oncol. *27,* 1660-1666.

Degterev, A., Boyce, M., and Yuan, J. (2003). A decade of caspases. Oncogene *22,* 8543-8567.

Desplanques, G., Giuliani, N., Delsignore, R., Rizzoli, V., Bataille, R., and Barille-Nion, S. (2009). Impact of XIAP protein levels on the survival of myeloma cells. Haematologica *94,* 87-93.

Dever, T.E. (2002). Gene-specific regulation by general translation factors. Cell *108,* 545-556.

Dever, T.E., Feng, L., Wek, R.C., Cigan, A.M., Donahue, T.F., and Hinnebusch, A.G. (1992). Phosphorylation of initiation factor 2 alpha by protein kinase GCN2 mediates gene-specific translational control of GCN4 in yeast. Cell *68,* 585-596.

Deveraux, Q.L., and Reed, J.C. (1999). IAP family proteins--suppressors of apoptosis. Genes Dev. *13,* 239-252.

Deveraux, Q.L., Roy, N., Stennicke, H.R., Van Arsdale, T., Zhou, Q., Srinivasula, S.M., Alnemri, E.S., Salvesen, G.S., and Reed, J.C. (1998). IAPs block apoptotic events induced by caspase-8 and cytochrome c by direct inhibition of distinct caspases. EMBO J. *17,* 2215-2223.

Deveraux, Q.L., Takahashi, R., Salvesen, G.S., and Reed, J.C. (1997). X-linked IAP is a direct inhibitor of cell-death proteases. Nature *388,* 300-304.

Dobson, T., Minic, A., Nielsen, K., Amiott, E., and Krushel, L. (2005). Internal initiation of translation of the TrkB mRNA is mediated by multiple regions within the 5' leader. Nucleic Acids Res. *33,* 2929-2941.

Du, C., Fang, M., Li, Y., Li, L., and Wang, X. (2000). Smac, a mitochondrial protein that promotes cytochrome c-dependent caspase activation by eliminating IAP inhibition. Cell *102,* 33-42.

Dumont, F.J., and Su, Q. (1996). Mechanism of action of the immunosuppressant rapamycin. Life Sci. *58,* 373-395.

Dyer, J.R., Michel, S., Lee, W., Castellucci, V.F., Wayne, N.L., and Sossin, W.S. (2003). An activity-dependent switch to cap-independent translation triggered by eIF4E dephosphorylation. Nat. Neurosci. *6,* 219-220.

Eckelman, B.P., and Salvesen, G.S. (2006). The human anti-apoptotic proteins cIAP1 and cIAP2 bind but do not inhibit caspases. J. Biol. Chem. *281,* 3254-3260.

Emamaullee, J.A., Rajotte, R.V., Liston, P., Korneluk, R.G., Lakey, J.R., Shapiro, A.M., and Elliott, J.F. (2005). XIAP overexpression in human islets prevents early posttransplant apoptosis and reduces the islet mass needed to treat diabetes. Diabetes *54,* 2541-2548.

Folkman, J. (1976). The vascularization of tumors. Sci. Am. *234,* 58-64, 70-3.

Fuentes-Prior, P., and Salvesen, G.S. (2004). The protein structures that shape caspase activity, specificity, activation and inhibition. Biochem. J. *384,* 201-232.

Futterer, J., Kiss-Laszlo, Z., and Hohn, T. (1993). Nonlinear ribosome migration on cauliflower mosaic virus 35S RNA. Cell *73,* 789-802.

Gebauer, F., and Hentze, M.W. (2004). Molecular mechanisms of translational control. Nat. Rev. Mol. Cell Biol. *5,* 827-835.

Gingras, A.C., Svitkin, Y., Belsham, G.J., Pause, A., and Sonenberg, N. (1996). Activation of the translational suppressor 4E-BP1 following infection with encephalomyocarditis virus and poliovirus. Proc. Natl. Acad. Sci. U. S. A. *93,* 5578-5583.

Goffredo, D., Rigamonti, D., Zuccato, C., Tartari, M., Valenza, M., and Cattaneo, E. (2005). Prevention of cytosolic IAPs degradation: a potential pharmacological target in Huntington's Disease. Pharmacol. Res. *52,* 140-150.

Gottfried, Y., Rotem, A., Lotan, R., Steller, H., and Larisch, S. (2004). The mitochondrial ARTS protein promotes apoptosis through targeting XIAP. EMBO J. *23,* 1627-1635.

Graber, T.E., and Holcik, M. (2007). Cap-independent regulation of gene expression in apoptosis. Mol. Biosyst *3,* 825-834.

Gross, A., McDonnell, J.M., and Korsmeyer, S.J. (1999). BCL-2 family members and the mitochondria in apoptosis. Genes Dev. *13,* 1899-1911.

Grunwald, V., DeGraffenried, L., Russel, D., Friedrichs, W.E., Ray, R.B., and Hidalgo, M. (2002). Inhibitors of mTOR reverse doxorubicin resistance conferred by PTEN status in prostate cancer cells. Cancer Res. *62,* 6141-6145.

Gu, L., Zhu, N., Zhang, H., Durden, D.L., Feng, Y., and Zhou, M. (2009). Regulation of XIAP translation and induction by MDM2 following irradiation. Cancer. Cell. *15,* 363-375.

Hamilton, T.L., Stoneley, M., Spriggs, K.A., and Bushell, M. (2006). TOPs and their regulation. Biochem. Soc. Trans. *34,* 12-16.

Hannon, G.J. (2002). RNA interference. Nature *418,* 244-251.

Hao, Q., Li, X., and Lu, X. (2007). Antisense oligonucleotides targeting XIAP induce apoptosis and enhance radiotherapeutic activity against hep-2 cells in vitro. Lin Chung Er Bi Yan Hou Tou Jing Wai Ke Za Zhi *21,* 970-972.

Hegde, R., Srinivasula, S.M., Zhang, Z., Wassell, R., Mukattash, R., Cilenti, L., DuBois, G., Lazebnik, Y., Zervos, A.S., Fernandes-Alnemri, T., and Alnemri, E.S. (2002). Identification of Omi/HtrA2 as a mitochondrial apoptotic serine protease that disrupts inhibitor of apoptosis protein-caspase interaction. J. Biol. Chem. *277,* 432-438.

Hellen, C.U., and Sarnow, P. (2001). Internal ribosome entry sites in eukaryotic mRNA molecules. Genes Dev. *15,* 1593-1612.

Henis-Korenblit, S., Shani, G., Sines, T., Marash, L., Shohat, G., and Kimchi, A. (2002). The caspase-cleaved DAP5 protein supports internal ribosome entry site-mediated translation of death proteins. Proc. Natl. Acad. Sci. U. S. A. *99,* 5400-5405.

Hershey, J.W. (1991). Translational control in mammalian cells. Annu. Rev. Biochem. *60,* 717-755.

Hershey, J.W., and Merrick, W.C. (2000). Translational Control of Gene Expression. Sonenberg, N., Hershey, J. W. and Mathews, B. M. B. eds., (New York, USA: Cold Spring Harbour Laboratory Press) pp. 33.

Hinnebusch, A.G. (2000). Translational Control of Gene Expression. Sonenberg, N., Hershey, J. W. and Mathews, B. M. B. eds., (New York, USA: Cold Spring Harbour Laboratory Press) pp. 185.

Hinnebusch, A.G. (1997). Translational regulation of yeast GCN4. A window on factors that control initiator-trna binding to the ribosome. J. Biol. Chem. *272,* 21661-21664.

Holcik, M. (2003). Translational upregulation of the X-linked inhibitor of apoptosis. Ann. N. Y. Acad. Sci. *1010,* 249-258.

Holcik, M., Gordon, B.W., and Korneluk, R.G. (2003). The internal ribosome entry site-mediated translation of antiapoptotic protein XIAP is modulated by the heterogeneous nuclear ribonucleoproteins C1 and C2. Mol. Cell. Biol. *23,* 280-288.

Holcik, M., Graber, T., Lewis, S.M., Lefebvre, C.A., Lacasse, E., and Baird, S. (2005). Spurious splicing within the XIAP 5' UTR occurs in the Rluc/Fluc but not the betagal/CAT bicistronic reporter system. RNA *11,* 1605-1609.

Holcik, M., and Korneluk, R.G. (2000). Functional characterization of the X-linked inhibitor of apoptosis (XIAP) internal ribosome entry site element: role of La autoantigen in XIAP translation. Mol. Cell. Biol. *20,* 4648-4657.

Holcik, M., Lefebvre, C., Yeh, C., Chow, T., and Korneluk, R.G. (1999). A new internal-ribosome-entry-site motif potentiates XIAP-mediated cytoprotection. Nat. Cell Biol. *1,* 190-192.

Holcik, M., Lefebvre, C.A., Hicks, K., and Korneluk, R.G. (2002). Cloning and characterization of the rat homologues of the Inhibitor of Apoptosis protein 1, 2, and 3 genes. BMC Genomics *3,* 5.

Holcik, M., and Sonenberg, N. (2005). Translational control in stress and apoptosis. Nat. Rev. Mol. Cell Biol. *6,* 318-327.

Holcik, M., Sonenberg, N., and Korneluk, R.G. (2000). Internal ribosome initiation of translation and the control of cell death. Trends Genet. *16,* 469-473.

Holcik, M., Yeh, C., Korneluk, R.G., and Chow, T. (2000). Translational upregulation of X-linked inhibitor of apoptosis (XIAP) increases resistance to radiation induced cell death. Oncogene *19,* 4174-4177.

Huang, H., Joazeiro, C.A., Bonfoco, E., Kamada, S., Leverson, J.D., and Hunter, T. (2000). The inhibitor of apoptosis, cIAP2, functions as a ubiquitin-protein ligase and

promotes in vitro monoubiquitination of caspases 3 and 7. J. Biol. Chem. *275,* 26661-26664.

Huang, Y., Park, Y.C., Rich, R.L., Segal, D., Myszka, D.G., and Wu, H. (2001). Structural basis of caspase inhibition by XIAP: differential roles of the linker versus the BIR domain. Cell *104,* 781-790.

Hughes, T.A. (2006). Regulation of gene expression by alternative untranslated regions. Trends Genet. *22,* 119-122.

Iacono, M., Mignone, F., and Pesole, G. (2005). uAUG and uORFs in human and rodent 5'untranslated mRNAs. Gene *349,* 97-105.

Jackson, R.J. (2005). Alternative mechanisms of initiating translation of mammalian mRNAs. Biochem. Soc. Trans. *33,* 1231-1241.

Jang, S.K., Krausslich, H.G., Nicklin, M.J., Duke, G.M., Palmenberg, A.C., and Wimmer, E. (1988). A segment of the 5' nontranslated region of encephalomyocarditis virus RNA directs internal entry of ribosomes during in vitro translation. J. Virol. *62,* 2636-2643.

Janowski, B.A., Younger, S.T., Hardy, D.B., Ram, R., Huffman, K.E., and Corey, D.R. (2007). Activating gene expression in mammalian cells with promoter-targeted duplex RNAs. Nat. Chem. Biol. *3,* 166-173.

Jefferies, H.B., Reinhard, C., Kozma, S.C., and Thomas, G. (1994). Rapamycin selectively represses translation of the "polypyrimidine tract" mRNA family. Proc. Natl. Acad. Sci. U. S. A. *91,* 4441-4445.

Jitrapakdee, S., Gong, Q., MacDonald, M.J., and Wallace, J.C. (1998). Regulation of rat pyruvate carboxylase gene expression by alternate promoters during development, in genetically obese rats and in insulin-secreting cells. Multiple transcripts with 5'-end heterogeneity modulate translation. J. Biol. Chem. *273,* 34422-34428.

Johnstone, O., and Lasko, P. (2001). Translational regulation and RNA localization in Drosophila oocytes and embryos. Annu. Rev. Genet. *35,* 365-406.

Karikari, C.A., Roy, I., Tryggestad, E., Feldmann, G., Pinilla, C., Welsh, K., Reed, J.C., Armour, E.P., Wong, J., Herman, J., Rakheja, D., and Maitra, A. (2007). Targeting the apoptotic machinery in pancreatic cancers using small-molecule antagonists of the X-linked inhibitor of apoptosis protein. Mol. Cancer. Ther. *6,* 957-966.

Kaufman, R.J. (2004). Regulation of mRNA translation by protein folding in the endoplasmic reticulum. Trends Biochem. Sci. *29,* 152-158.

Kozak, M. (2001). New ways of initiating translation in eukaryotes? Mol. Cell. Biol. *21,* 1899-1907.

Kozak, M. (1989a). Circumstances and mechanisms of inhibition of translation by secondary structure in eucaryotic mRNAs. Mol. Cell. Biol. *9,* 5134-5142.

Kozak, M. (1989b). The scanning model for translation: an update. J. Cell Biol. *108,* 229-241.

Kozak, M. (1987a). At least six nucleotides preceding the AUG initiator codon enhance translation in mammalian cells. J. Mol. Biol. *196,* 947-950.

Kozak, M. (1987b). Effects of intercistronic length on the efficiency of reinitiation by eucaryotic ribosomes. Mol. Cell. Biol. *7,* 3438-3445.

Kozak, M. (1986). Bifunctional messenger RNAs in eukaryotes. Cell *47,* 481-483.

Kozak, M. (1983). Comparison of initiation of protein synthesis in procaryotes, eucaryotes, and organelles. Microbiol. Rev. *47,* 1-45.

Kumar, S. (2007). Caspase function in programmed cell death. Cell Death Differ. *14,* 32-43.

Kuwana, T., and Newmeyer, D.D. (2003). Bcl-2-family proteins and the role of mitochondria in apoptosis. Curr. Opin. Cell Biol. *15,* 691-699.

Lewis, S.M., and Holcik, M. (2005). IRES in distress: translational regulation of the inhibitor of apoptosis proteins XIAP and HIAP2 during cell stress. Cell Death Differ. *12,* 547-553.

Lewis, S.M., Veyrier, A., Hosszu Ungureanu, N., Bonnal, S., Vagner, S., and Holcik, M. (2007). Subcellular Relocalization of a Trans-acting Factor Regulates XIAP IRES-dependent Translation. Mol. Biol. Cell *18,* 1302-1311.

Li, L.-C., Okino, S.T., Zhao, H., Pookot, D., Place, R.F., Urakami, S., Enokida, H., Dahiya, R. (2006). Small dsRNAs induce transcriptional activation in human cells. Proc. Natl. Acad. Sci. U. S. A. *103,* 17337-17342.

Li, P., Nijhawan, D., Budihardjo, I., Srinivasula, S.M., Ahmad, M., Alnemri, E.S., and Wang, X. (1997). Cytochrome c and dATP-dependent formation of Apaf-1/caspase-9 complex initiates an apoptotic protease cascade. Cell *91,* 479-489.

Li, X., Yang, Y., and Ashwell, J.D. (2002). TNF-RII and c-IAP1 mediate ubiquitination and degradation of TRAF2. Nature *416,* 345-347.

Liston, P., Roy, N., Tamai, K., Lefebvre, C., Baird, S., Cherton-Horvat, G., Farahani, R., McLean, M., Ikeda, J.E., MacKenzie, A., and Korneluk, R.G. (1996). Suppression of apoptosis in mammalian cells by NAIP and a related family of IAP genes. Nature *379,* 349-353.

Lopez-Lastra, M., Rivas, A., and Barria, M.I. (2005). Protein synthesis in eukaryotes: the growing biological relevance of cap-independent translation initiation. Biol. Res. *38,* 121-146.

Lotocki, G., and Keane, R.W. (2002). Inhibitors of apoptosis proteins in injury and disease. IUBMB Life *54,* 231-240.

Lu, M., Lin, S.C., Huang, Y., Kang, Y.J., Rich, R., Lo, Y.C., Myszka, D., Han, J., and Wu, H. (2007). XIAP induces NF-kappaB activation via the BIR1/TAB1 interaction and BIR1 dimerization. Mol. Cell *26,* 689-702.

Lyn, D., Bao, S., Bennett, N.A., Liu, X., and Emmett, N.L. (2002). Ischemia elicits a coordinated expression of pro-survival proteins in mouse myocardium. ScientificWorldJournal *2,* 997-1003.

MacGregor, G.R., Nolan, G.P., Fiering, S., Roederer, M., and Herzenberg, L.A. (1991). Methods in Molecular Biology (Clifton, New Jersey: Humana).

Marcotrigiano, J., Gingras, A.C., Sonenberg, N., and Burley, S.K. (1997). Cocrystal structure of the messenger RNA 5' cap-binding protein (eIF4E) bound to 7-methyl-GDP. Cell *89,* 951-961.

Marissen, W.E., and Lloyd, R.E. (1998). Eukaryotic translation initiation factor 4G is targeted for proteolytic cleavage by caspase 3 during inhibition of translation in apoptotic cells. Mol. Cell. Biol. *18,* 7565-7574.

Martineau, Y., Le Bec, C., Monbrun, L., Allo, V., Chiu, I.M., Danos, O., Moine, H., Prats, H., and Prats, A.C. (2004). Internal ribosome entry site structural motifs conserved among mammalian fibroblast growth factor 1 alternatively spliced mRNAs. Mol. Cell. Biol. *24,* 7622-7635.

Martins, L.M., Iaccarino, I., Tenev, T., Gschmeissner, S., Totty, N.F., Lemoine, N.R., Savopoulos, J., Gray, C.W., Creasy, C.L., Dingwall, C., and Downward, J. (2002). The serine protease Omi/HtrA2 regulates apoptosis by binding XIAP through a reaper-like motif. J. Biol. Chem. *277,* 439-444.

Mathews, B.M.B., Sonenberg, N., and Hershey, J.W. (2000). Translational Control of Gene Expression. Sonenberg, N., Hershey, J. W. and Mathews, B. M. B. eds., (New York, USA: Cold Spring Harbour Laboratory Press) pp. 1.

McDade, S.S., Hall, P.A., and Russell, S.E. (2007). Translational control of SEPT9 isoforms is perturbed in disease. Hum. Mol. Genet. *16,* 742-752.

Miller, L.K. (1999). An exegesis of IAPs: salvation and surprises from BIR motifs. Trends Cell Biol. *9,* 323-328.

Mitchell, S.A., Spriggs, K.A., Bushell, M., Evans, J.R., Stoneley, M., Le Quesne, J.P., Spriggs, R.V., and Willis, A.E. (2005). Identification of a motif that mediates polypyrimidine tract-binding protein-dependent internal ribosome entry. Genes Dev. *19,* 1556-1571.

Mizrachy-Schwartz, S., Kravchenko-Balasha, N., Ben-Bassat, H., Klein, S., and Levitzki, A. (2007). Optimization of energy-consuming pathways towards rapid growth in HPV-transformed cells. PLoS ONE *2,* e628.

Mokrejs, M., Vopalensky, V., Kolenaty, O., Masek, T., Feketova, Z., Sekyrova, P., Skaloudova, B., Kriz, V., and Pospisek, M. (2006). IRESite: the database of experimentally verified IRES structures (www.iresite.org). Nucleic Acids Res. *34,* D125-30.

Morishima, N., Nakanishi, K., Takenouchi, H., Shibata, T., and Yasuhiko, Y. (2002). An endoplasmic reticulum stress-specific caspase cascade in apoptosis. Cytochrome c-independent activation of caspase-9 by caspase-12. J. Biol. Chem. *277,* 34287-34294.

Morley, S.J., Coldwell, M.J., and Clemens, M.J. (2005). Initiation factor modifications in the preapoptotic phase. Cell Death Differ. *12,* 571-584.

Morley, S.J., McKendrick, L., and Bushell, M. (1998). Cleavage of translation initiation factor 4G (eIF4G) during anti-Fas IgM-induced apoptosis does not require signalling through the p38 mitogen-activated protein (MAP) kinase. FEBS Lett. *438,* 41-48.

Morris, D.R., and Geballe, A.P. (2000). Upstream open reading frames as regulators of mRNA translation. Mol. Cell. Biol. *20,* 8635-8642.

Neshat, M.S., Mellinghoff, I.K., Tran, C., Stiles, B., Thomas, G., Petersen, R., Frost, P., Gibbons, J.J., Wu, H., and Sawyers, C.L. (2001). Enhanced sensitivity of PTEN-deficient tumors to inhibition of FRAP/mTOR. Proc. Natl. Acad. Sci. U. S. A. *98,* 10314-10319.

Nevins, T.A., Harder, Z.M., Korneluk, R.G., and Holcik, M. (2003). Distinct regulation of internal ribosome entry site-mediated translation following cellular stress is mediated by apoptotic fragments of eIF4G translation initiation factor family members eIF4GI and p97/DAP5/NAT1. J. Biol. Chem. *278,* 3572-3579.

Oyadomari, S., and Mori, M. (2004). Roles of CHOP/GADD153 in endoplasmic reticulum stress. Cell Death Differ. *11,* 381-389.

Pelletier, J., and Sonenberg, N. (1988). Internal initiation of translation of eukaryotic mRNA directed by a sequence derived from poliovirus RNA. Nature *334,* 320-325.

Pestova, T.V., Borukhov, S.I., and Hellen, C.U. (1998). Eukaryotic ribosomes require initiation factors 1 and 1A to locate initiation codons. Nature *394,* 854-859.

Pestova, T.V., and Kolupaeva, V.G. (2002). The roles of individual eukaryotic translation initiation factors in ribosomal scanning and initiation codon selection. Genes Dev. *16,* 2906-2922.

Pestova, T.V., Kolupaeva, V.G., Lomakin, I.B., Pilipenko, E.V., Shatsky, I.N., Agol, V.I., and Hellen, C.U. (2001). Molecular mechanisms of translation initiation in eukaryotes. Proc. Natl. Acad. Sci. U. S. A. *98,* 7029-7036.

Pickering, B.M., Mitchell, S.A., Evans, J.R., and Willis, A.E. (2003). Polypyrimidine tract binding protein and poly r(C) binding protein 1 interact with the BAG-1 IRES and stimulate its activity in vitro and in vivo. Nucleic Acids Res. *31,* 639-646.

Pickering, B.M., Mitchell, S.A., Spriggs, K.A., Stoneley, M., and Willis, A.E. (2004). Bag-1 internal ribosome entry segment activity is promoted by structural changes mediated by poly(rC) binding protein 1 and recruitment of polypyrimidine tract binding protein 1. Mol. Cell. Biol. *24,* 5595-5605.

Pickering, B.M., and Willis, A.E. (2005). The implications of structured 5' untranslated regions on translation and disease. Semin. Cell Dev. Biol. *16,* 39-47.

Podsypanina, K., Lee, R.T., Politis, C., Hennessy, I., Crane, A., Puc, J., Neshat, M., Wang, H., Yang, L., Gibbons, J. *et al.* (2001). An inhibitor of mTOR reduces neoplasia and normalizes p70/S6 kinase activity in Pten+/- mice. Proc. Natl. Acad. Sci. U. S. A. *98,* 10320-10325.

Porter, A.G., and Janicke, R.U. (1999). Emerging roles of caspase-3 in apoptosis. Cell Death Differ. *6,* 99-104.

Pozner, A., Goldenberg, D., Negreanu, V., Le, S.Y., Elroy-Stein, O., Levanon, D., and Groner, Y. (2000). Transcription-coupled translation control of AML1/RUNX1 is mediated by cap- and internal ribosome entry site-dependent mechanisms. Mol. Cell. Biol. *20,* 2297-2307.

Prevot, D., Darlix, J.L., and Ohlmann, T. (2003). Conducting the initiation of protein synthesis: the role of eIF4G. Biol. Cell. *95,* 141-156.

Price, N.T., and Proud, C.G. (1990). Phosphorylation of protein synthesis initiation factor-2. Identification of the site in the alpha-subunit phosphorylated in reticulocyte lysates. Biochim. Biophys. Acta *1054,* 83-88.

Proud, C.G. (2005). eIF2 and the control of cell physiology. Semin. Cell Dev. Biol. *16,* 3-12.

Pruitt, K.D., Tatusova, T., and Maglott, D.R. (2007). NCBI reference sequences (RefSeq): a curated non-redundant sequence database of genomes, transcripts and proteins. Nucleic Acids Res. *35,* D61-5.

Pyronnet, S., Dostie, J., and Sonenberg, N. (2001). Suppression of cap-dependent translation in mitosis. Genes Dev. *15,* 2083-2093.

Rami, A., Agarwal, R., and Spahn, A. (2007). Synergetic effects of caspase 3 and mu-calpain in XIAP-breakdown upon focal cerebral ischemia. Neurochem. Res. *32,* 2072-2079.

Rao, R.V., Ellerby, H.M., and Bredesen, D.E. (2004). Coupling endoplasmic reticulum stress to the cell death program. Cell Death Differ. *11,* 372-380.

Riedl, S.J., Renatus, M., Schwarzenbacher, R., Zhou, Q., Sun, C., Fesik, S.W., Liddington, R.C., and Salvesen, G.S. (2001). Structural basis for the inhibition of caspase-3 by XIAP. Cell *104,* 791-800.

Rigaud, S., Fondaneche, M.C., Lambert, N., Pasquier, B., Mateo, V., Soulas, P., Galicier, L., Le Deist, F., Rieux-Laucat, F., Revy, P. *et al.* (2006). XIAP deficiency in humans causes an X-linked lymphoproliferative syndrome. Nature *444,* 110-114.

Rudra, D., and Warner, J.R. (2004). What better measure than ribosome synthesis? Genes Dev. *18,* 2431-2436.

Sachs, A.B. (2000). Cell cycle-dependent translation initiation: IRES elements prevail. Cell *101,* 243-245.

Salvesen, G.S., and Duckett, C.S. (2002). IAP proteins: blocking the road to death's door. Nat. Rev. Mol. Cell Biol. *3,* 401-410.

Samuel, T., Welsh, K., Lober, T., Togo, S.H., Zapata, J.M., and Reed, J.C. (2006). Distinct BIR domains of cIAP1 mediate binding to and ubiquitination of tumor necrosis factor receptor-associated factor 2 and second mitochondrial activator of caspases. J. Biol. Chem. *281,* 1080-1090.

Scarabelli, T.M., Stephanou, A., Pasini, E., Gitti, G., Townsend, P., Lawrence, K., Chen-Scarabelli, C., Saravolatz, L., Latchman, D., Knight, R., and Gardin, J. (2004). Minocycline inhibits caspase activation and reactivation, increases the ratio of XIAP to smac/DIABLO, and reduces the mitochondrial leakage of cytochrome C and smac/DIABLO. J. Am. Coll. Cardiol. *43,* 865-874.

Schmelzle, T., and Hall, M.N. (2000). TOR, a central controller of cell growth. Cell *103,* 253-262.

Scott, F.L., Denault, J.B., Riedl, S.J., Shin, H., Renatus, M., and Salvesen, G.S. (2005). XIAP inhibits caspase-3 and -7 using two binding sites: evolutionarily conserved mechanism of IAPs. EMBO J. *24,* 645-655.

Sehgal, S.N. (1998). Rapamune (RAPA, rapamycin, sirolimus): mechanism of action immunosuppressive effect results from blockade of signal transduction and inhibition of cell cycle progression. Clin. Biochem. *31,* 335-340.

Shamji, A.F., Nghiem, P., and Schreiber, S.L. (2003). Integration of growth factor and nutrient signaling: implications for cancer biology. Mol. Cell *12,* 271-280.

Shaw, T.J., Lacasse, E.C., Durkin, J.P., and Vanderhyden, B.C. (2008). Downregulation of XIAP expression in ovarian cancer cells induces cell death in vitro and in vivo. Int. J. Cancer *122,* 1430-1434.

Shi, Y. (2002). Mechanisms of caspase activation and inhibition during apoptosis. Mol. Cell *9,* 459-470.

Shi, Y., Frankel, A., Radvanyi, L.G., Penn, L.Z., Miller, R.G., and Mills, G.B. (1995). Rapamycin enhances apoptosis and increases sensitivity to cisplatin in vitro. Cancer Res. *55,* 1982-1988.

Shiozaki, E.N., Chai, J., Rigotti, D.J., Riedl, S.J., Li, P., Srinivasula, S.M., Alnemri, E.S., Fairman, R., and Shi, Y. (2003). Mechanism of XIAP-mediated inhibition of caspase-9. Mol. Cell *11,* 519-527.

Silke, J., Kratina, T., Chu, D., Ekert, P.G., Day, C.L., Pakusch, M., Huang, D.C., and Vaux, D.L. (2005). Determination of cell survival by RING-mediated regulation of inhibitor of apoptosis (IAP) protein abundance. Proc. Natl. Acad. Sci. U. S. A. *102,* 16182-16187.

Simons, M., Beinroth, S., Gleichmann, M., Liston, P., Korneluk, R.G., MacKenzie, A.E., Bahr, M., Klockgether, T., Robertson, G.S., Weller, M., and Schulz, J.B. (1999). Adenovirus-mediated gene transfer of inhibitors of apoptosis protein delays apoptosis in cerebellar granule neurons. J. Neurochem. *72,* 292-301.

Sonenberg, N., and Dever, T.E. (2003). Eukaryotic translation initiation factors and regulators. Curr. Opin. Struct. Biol. *13,* 56-63.

Spahn, A., Blondeau, N., Heurteaux, C., Dehghani, F., and Rami, A. (2008). Concomitant Transitory Up-Regulation of X-Linked Inhibitor of Apoptosis Protein (XIAP) and the Heterogeneous Nuclear Ribonucleoprotein C1-C2 in Surviving Cells During Neuronal Apoptosis. Neurochem. Res. *33,* 1859-68.

Spriggs, K.A., Bushell, M., Mitchell, S.A., and Willis, A.E. (2005). Internal ribosome entry segment-mediated translation during apoptosis: the role of IRES-trans-acting factors. Cell Death Differ. *12,* 585-591.

Spriggs, K.A., Cobbold, L.C., Jopling, C.L., Cooper, R.E., Wilson, L.A., Stoneley, M., Coldwell, M.J., Poncet, D., Shen, Y.C., Morley, S.J., Bushell, M., and Willis, A.E. (2009). Canonical initiation factor requirements of the Myc family of internal ribosome entry segments. Mol. Cell. Biol. *29,* 1565-1574.

Spriggs, K.A., Stoneley, M., Bushell, M., and Willis, A.E. (2008). Re-programming of translation following cell stress allows IRES-mediated translation to predominate. Biol. Cell. *100,* 27-38.

Srinivasula, S.M., Hegde, R., Saleh, A., Datta, P., Shiozaki, E., Chai, J., Lee, R.A., Robbins, P.D., Fernandes-Alnemri, T., Shi, Y., and Alnemri, E.S. (2001). A conserved XIAP-interaction motif in caspase-9 and Smac/DIABLO regulates caspase activity and apoptosis. Nature *410,* 112-116.

Stoneley, M., Chappell, S.A., Jopling, C.L., Dickens, M., MacFarlane, M., and Willis, A.E. (2000). c-Myc protein synthesis is initiated from the internal ribosome entry segment during apoptosis. Mol. Cell. Biol. *20,* 1162-1169.

Sun, C., Cai, M., Meadows, R.P., Xu, N., Gunasekera, A.H., Herrmann, J., Wu, J.C., and Fesik, S.W. (2000). NMR structure and mutagenesis of the third Bir domain of the inhibitor of apoptosis protein XIAP. J. Biol. Chem. *275,* 33777-33781.

Suzuki, Y., Imai, Y., Nakayama, H., Takahashi, K., Takio, K., and Takahashi, R. (2001). A serine protease, HtrA2, is released from the mitochondria and interacts with XIAP, inducing cell death. Mol. Cell *8,* 613-621.

Tamm, I. (2008). AEG-35156, an antisense oligonucleotide against X-linked inhibitor of apoptosis for the potential treatment of cancer. Curr. Opin. Investig Drugs *9,* 638-646.

Tamm, I., Kornblau, S.M., Segall, H., Krajewski, S., Welsh, K., Kitada, S., Scudiero, D.A., Tudor, G., Qui, Y.H., Monks, A., Andreeff, M., and Reed, J.C. (2000). Expression and prognostic significance of IAP-family genes in human cancers and myeloid leukemias. Clin. Cancer Res. *6,* 1796-1803.

Tenev, T., Zachariou, A., Wilson, R., Ditzel, M., and Meier, P. (2005). IAPs are functionally non-equivalent and regulate effector caspases through distinct mechanisms. Nat. Cell Biol. *7,* 70-77.

Tesfay, M.Z., Yin, J., Gardner, C.L., Khoretonenko, M.V., Korneeva, N.L., Rhoads, R.E., Ryman, K.D., and Klimstra, W.B. (2008). Alpha/beta interferon inhibits cap-dependent translation of viral but not cellular mRNA by a PKR-independent mechanism. J. Virol. *82,* 2620-2630.

Thermann, R., and Hentze, M.W. (2007). Drosophila miR2 induces pseudo-polysomes and inhibits translation initiation. Nature *447,* 875-878.

Thomlinson, R.H., and Gray, L.H. (1955). The histological structure of some human lung cancers and the possible implications for radiotherapy. Br. J. Cancer *9,* 539-549.

Thornberry, N.A., and Lazebnik, Y. (1998). Caspases: enemies within. Science *281,* 1312-1316.

Tokuda, E., Ono, S., Ishige, K., Watanabe, S., Okawa, E., Ito, Y., and Suzuki, T. (2007). Dysequilibrium between caspases and their inhibitors in a mouse model for amyotrophic lateral sclerosis. Brain Res. *1148,* 234-242.

Uren, A.G., Coulson, E.J., and Vaux, D.L. (1998). Conservation of baculovirus inhibitor of apoptosis repeat proteins (BIRPs) in viruses, nematodes, vertebrates and yeasts. Trends Biochem. Sci. *23,* 159-162.

Van Eden, M.E., Byrd, M.P., Sherrill, K.W., and Lloyd, R.E. (2004a). Demonstrating internal ribosome entry sites in eukaryotic mRNAs using stringent RNA test procedures. RNA *10,* 720-730.

Van Eden, M.E., Byrd, M.P., Sherrill, K.W., and Lloyd, R.E. (2004b). Translation of cellular inhibitor of apoptosis protein 1 (c-IAP1) mRNA is IRES mediated and regulated during cell stress. RNA *10,* 469-481.

van Loo, G., van Gurp, M., Depuydt, B., Srinivasula, S.M., Rodriguez, I., Alnemri, E.S., Gevaert, K., Vandekerckhove, J., Declercq, W., and Vandenabeele, P. (2002). The serine protease Omi/HtrA2 is released from mitochondria during apoptosis. Omi interacts with

caspase-inhibitor XIAP and induces enhanced caspase activity. Cell Death Differ. *9,* 20-26.

Vander Heiden, M.G., and Thompson, C.B. (1999). Bcl-2 proteins: regulators of apoptosis or of mitochondrial homeostasis? Nat. Cell Biol. *1,* E209-16.

Varfolomeev, E., Blankenship, J.W., Wayson, S.M., Fedorova, A.V., Kayagaki, N., Garg, P., Zobel, K., Dynek, J.N., Elliott, L.O., Wallweber, H.J. *et al.* (2007). IAP antagonists induce autoubiquitination of c-IAPs, NF-kappaB activation, and TNFalpha-dependent apoptosis. Cell *131,* 669-681.

Varfolomeev, E., Wayson, S.M., Dixit, V.M., Fairbrother, W.J., and Vucic, D. (2006). The inhibitor of apoptosis protein fusion c-IAP2.MALT1 stimulates NF-kappaB activation independently of TRAF1 AND TRAF2. J. Biol. Chem. *281,* 29022-29029.

Vaux, D.L., and Silke, J. (2005). IAPs, RINGs and ubiquitylation. Nat. Rev. Mol. Cell Biol. *6,* 287-297.

Verhagen, A.M., Coulson, E.J., and Vaux, D.L. (2001). Inhibitor of apoptosis proteins and their relatives: IAPs and other BIRPs. Genome Biol. *2,* Reviews3009.

Verhagen, A.M., Ekert, P.G., Pakusch, M., Silke, J., Connolly, L.M., Reid, G.E., Moritz, R.L., Simpson, R.J., and Vaux, D.L. (2000). Identification of DIABLO, a mammalian protein that promotes apoptosis by binding to and antagonizing IAP proteins. Cell *102,* 43-53.

Verhagen, A.M., Silke, J., Ekert, P.G., Pakusch, M., Kaufmann, H., Connolly, L.M., Day, C.L., Tikoo, A., Burke, R., Wrobel, C. *et al.* (2002). HtrA2 promotes cell death through its serine protease activity and its ability to antagonize inhibitor of apoptosis proteins. J. Biol. Chem. *277,* 445-454.

Vince, J.E., Wong, W.W., Khan, N., Feltham, R., Chau, D., Ahmed, A.U., Benetatos, C.A., Chunduru, S.K., Condon, S.M., McKinlay, M. *et al.* (2007). IAP antagonists target cIAP1 to induce TNFalpha-dependent apoptosis. Cell *131,* 682-693.

Wang, G., Guo, X., Silveyra, P., Kimball, S.R., and Floros, J. (2009). Cap-independent translation of human SP-A 5'-UTR variants: a double-loop structure and cis-element contribution. Am. J. Physiol. Lung Cell. Mol. Physiol. *296,* L635-47.

Warner, J.R. (1999). The economics of ribosome biosynthesis in yeast. Trends Biochem. Sci. *24,* 437-440.

Wimmer, E. (1982). Genome-linked proteins of viruses. Cell *28,* 199-201.

Wyllie, A.H. (1981). *Cell death: a new classification separating apoptosis from necrosis..* In *Cell Death in Biology and Pathology*, Bowen, I. D., and Lockshin, R. A. eds., (London: Chapman & Hall) pp. 9.

Yan, H., Frost, P., Shi, Y., Hoang, B., Sharma, S., Fisher, M., Gera, J., and Lichtenstein, A. (2006). Mechanism by which mammalian target of rapamycin inhibitors sensitize multiple myeloma cells to dexamethasone-induced apoptosis. Cancer Res. *66,* 2305-2313.

Yang, D., Buchholz, F., Huang, Z., Goga, A., Chen, C.Y., Brodsky, F.M., and Bishop, J.M. (2002). Short RNA duplexes produced by hydrolysis with Escherichia coli RNase III mediate effective RNA interference in mammalian cells. Proc. Natl. Acad. Sci. U. S. A. *99,* 9942-9947.

Yang, Y., Fang, S., Jensen, J.P., Weissman, A.M., and Ashwell, J.D. (2000). Ubiquitin protein ligase activity of IAPs and their degradation in proteasomes in response to apoptotic stimuli. Science *288,* 874-877.

Yoon, A., Peng, G., Brandenburger, Y., Zollo, O., Xu, W., Rego, E., and Ruggero, D. (2006). Impaired control of IRES-mediated translation in X-linked dyskeratosis congenita. Science *312,* 902-906.

Yueh, A., and Schneider, R.J. (2000). Translation by ribosome shunting on adenovirus and hsp70 mRNAs facilitated by complementarity to 18S rRNA. Genes Dev. *14,* 414-421.

Yueh, A., and Schneider, R.J. (1996). Selective translation initiation by ribosome jumping in adenovirus-infected and heat-shocked cells. Genes Dev. *10,* 1557-1567.

Zhao, X., Chen, J., Lei, L., Hu, G., Xiong, Y., Xu, J., Li, Q., Yang, X., Chang, C.C., Song, B., Chang, T., and Li, B. (2009). The optional long 5'-untranslated region of human ACAT1 mRNAs impairs the production of ACAT1 protein by promoting its mRNA decay. Acta Biochim. Biophys. Sin. (Shanghai) *41,* 30-41.

Contributions of Collaborators

Bioinformatic identification and organization of the XIAP mRNA isoforms by Dr. Stephen Baird

HF1 cell lines were generous gifts from Dr. Alexander Levitzki

Appendix I

XIAP UTR sequences:

Long UTR (L-UTR)[2]:

1 TGCCTGTTGT CCCAGTGTGA TTATTACTAG TGTAATTTTT CACTTTGAGA
51 AGTGTCCAGG TTTGGAGGAT AAATTATCTT TCTAATAATT GATACCCTTC
101 TCATAACCTA ACGGGTTCCT TTTAGTATTT TATCTGGGTT AAAATTACCA
151 GCTGTAATTT GGCAGCTCTA ATAAGACTGC AGCAATACTT ATCTTCCATT
201 TGAACAGATT GTTACTTGAC CAAGGGAAGT TAATAGCAAA AGTAACTGCA
251 GGGCACATGT ATGTCATGGG CAAAAAAAAA AAAAAAAGTA ACAGCAATTA
301 AGGTTTGCAG GTACTTAGAA TTTTTCCTGA GCCACCCTCT AGAGGGCAGT
351 GTTACATATA TATCTGTAAT TATCCAGTTA CAACAAAAAA AGGGCTCTCA
401 TTCATGCATG AAAATCAGAA ATATTTCATA CTCTTAAAGA ACACATTGGA
451 ACCAATATTA TGATTAAAAC ATATTTTGCT AAGCAAAGAG ATATTAAAAA
501 TTAATTCATT AACATTCTGA ACATTTTTTA ACTTGTAAAA ACAACTTTGA
551 TGCCTTGAAT ATATAATGAT TCATTATAAC AATTATGCAT AGATTTTAAT
601 AATCTGCATA TTTTATGCTT TCATGTTTTT CCTAATTAAT GATTTGACAT
651 GGTTAATAAT TATAATATAT TCTGCATCAC AGTTTACATA TTTATGTAAA
701 ATAAGCATTT AAAAATTATT AGTTTTATTC TGCCTGCTTA AATATTACTT
751 TCCTCAAAAA GAGAAAACAA AAATGCTAGA TTTTACTTTA TGACTTGAAT
801 GATGTGGTAA TGTCGAACTC TAGTATTTAG AATTAGAATG TTTCTTAGCG
851 GTCGTGTAGT TATTTTTATG TCATAAGTGG ATAATTTGTT AGCTCCTATA
901 ACAAAAGTCT GTTGCTTGTG TTTCACATTT TGGATTTCCT AATATAATGT
951 TCTCTTTTTA GAAAAGGTGG ACAAGTCCTA TTTTCAAGAG AAGATGACTT
1001 T

Short UTR (S-UTR):

1 TGACGGACCG CGCCCGGTGT CTCTTTGAGG CCCTGACGTG GACACACTTC
51 GGGTTTCACG ACTCCGGGTT TCTCCAGGGG ATGGGCCGGC CGGTAGAGGC
101 GCGTGAGGGA GACGAAGGGA CTTCCGTTTC CTTCACCTAG GCTGGGGCCA
151 AGCCGCAGAG CGGAGTTGGC ATTTCCAGAT TGGGGCTCGG GCCGCGCCTC
201 CTCCGGGACC CTCCCCTTGG ACCGAGCCGA TCGCCGCGGG GCAGTTCGGG
251 CCGGCTGTCC TGGCGCGAAA AGGTGGACAA GTCCTATTTT CAAGAGAAG

Hairpin structure:
(ΔG=-38 kcal/mol)

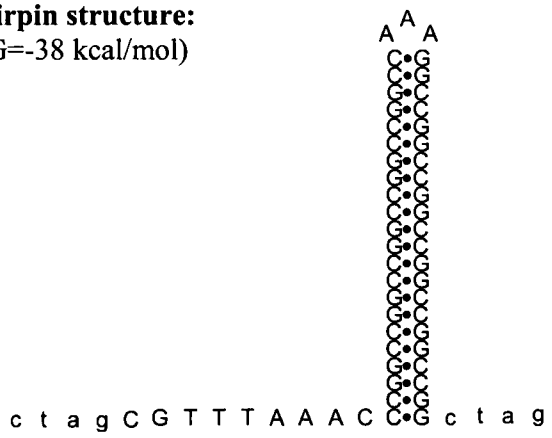

[2]This is the full-length UTR as used here.

Appendix II

Oligonucleotide sequences:

BCHP-1: 5' /5Phos/CTAGC**GTTTAAAC**CCGGCCGGCCGGCCGGCCGGCCAAA GGCCGGCCGGCCGGCCGGCCGG 3'
BCHP-2: 5' /5Phos/CTAGCCGGCCGGCCGGCCGGCCGGCCTTTGGCCGGCCG GCCGGCCGGC**CGGGTTTA**AACG 3'
qCAT5: 5' GCGTGTTACGGTGAAAACCT 3'
qCAT3: 5' GGGCGAAGAAGTTGTCCATA 3'
qNEO5 5' TGAATGAACTGCAGGACGAG 3'
qNEO3 5' CAATAGCAGCCAGTCCCTTC 3'
qGAL-F: 5' ACTATCCCGACCGCCTTACT 3'
qGAL-R: 5' CTGTAGGGGCTGATGTTGAA 3'
qActin-F: 5' CTGGAACGGTGAAGGTGACA 3'
qActin-R: 5' AAGGGACTTCCTGTAACAATGCA 3'
qGAPDH-F: 5' ACAGTCAGCCGCATCTTCTT 3'
qGAPDH-R: 5' ACGACCAAATCCGTTGACTC 3'
XIAPCDS-F (C1): 5' GCGGTGCTTTAGTTGTCAT 3'
XIAPCDS-R (C2): 5' TCGGGTATATGGTGTCTGATA 3'
CHEOXIRES-F (L1): 5' TTTTATTCTGCCTGCTTAAAT 3'
REFSEQXUTR-F (S1): 5' TCGGGCCGGCTGTCCT 3'
q4496-F: 5'AGGGCACATGTATGTCATGG 3'
q4496-R: 5' TAGAGGGTGGCTCAGGAAAA 3'
q323-F: 5' CTTCCGTTTCCTTCACCTA 3'
q323-R: 5' TAGGACTTGTCCACCTTTTC 3'
T7-F: 5' TCTAGATAATACGACTCACTATAGGG 3'
NT4-R: 5' TTTTTTTTTTTTTTTTTTTTTTTTTTTTTTTGGATCCTTACGCCCC GCCCTGCC 3'
4438-R: CTGAAATGCCTCAAAATGTTC
4405XhoI: 5'GAGCTCGAAGAGAACTTTTATCCTG 3'
4571NheI: 5'GCTAGCAATTAGAATGTTTCTTAGCGGTC 3'
350NheI: 5'GCTAGCTTCTGCATCACAGTTTAC 3'
NheI-4496: GCTAGCCCAGGTTTGCCTCATAACTAG

siRNA
XIAP IRES 751: r(AGGUUUGGAGGAUAAAUUA)dTdT
stealth 62: GCCGGCTGTCCTGGCGCGAAA
stealth 172: AAGGGACTTCCGTTTCCTTCA

GCTAGC : NheI restriction site
GTTTAAAC : PmeI restriction site
GAGCTC : XhoI restriction site

Appendix III

Vector map of pBicmod (containing the full length Long UTR):

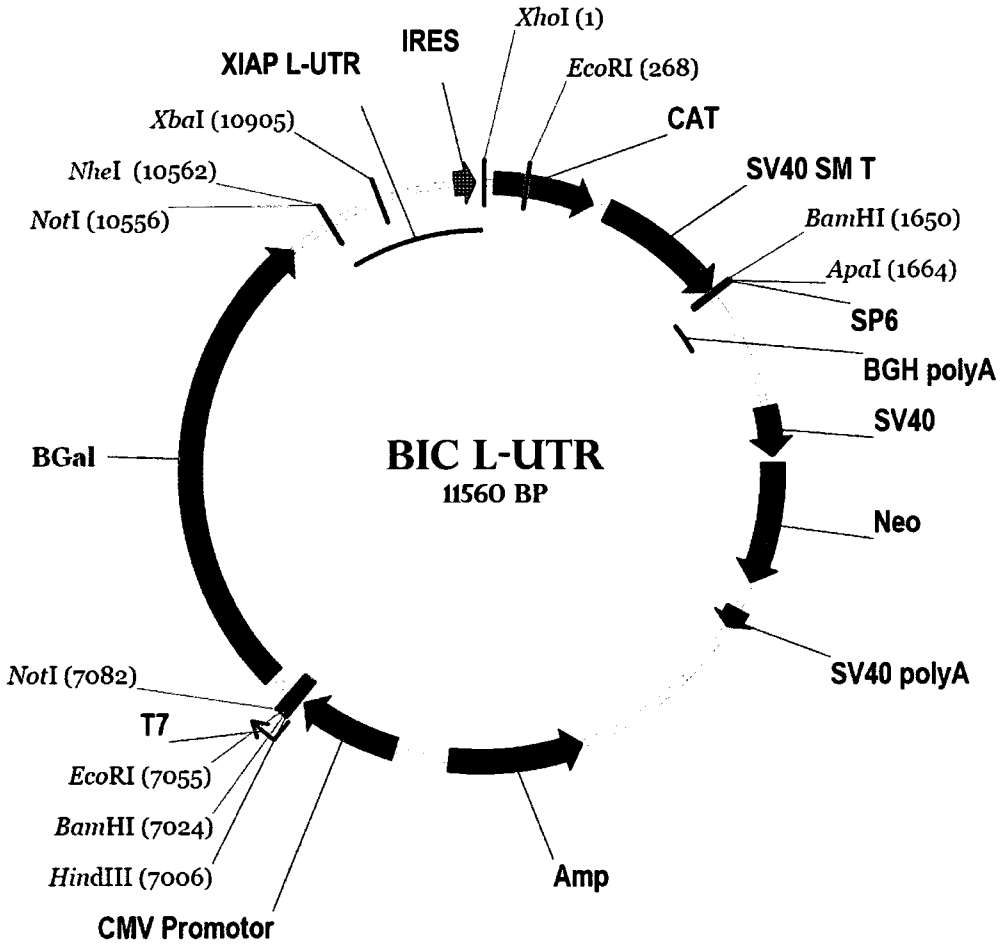

Curriculum Vitae

Education History

09/2007-present	M.Sc. Biochemistry, Specialization in Human & Molecular Genetics. University of Ottawa
09/2003-05/2007	B.Sc. Honours Biochemistry with Co-operative Education. University of Ottawa. Graduated *magna cum laude*.
09/2002-05/2003	B.Sc. Honours Biochemistry, Biotechnology with Co-operative Education. University of Ottawa
09/1997-06/2002	Ontario Secondary School Diploma. Graduated as an Ontario Scholar. Stouffville District Secondary School.

Research Experience

09/2007-present	M.Sc. Candidate. Apoptosis Research Centre. Characterization of translational modulation of X-linked Inhibitor of Apoptosis (XIAP) protein levels by alternate non-coding regions. Children's Hospital of Eastern Ontario, Ottawa.
05/2006-08/2007	Research Student. Apoptosis Research Centre. Examination of modes of translation used by X-linked Inhibitor of Apoptosis (XIAP) transcripts. Children's Hospital of Eastern Ontario, Ottawa.
01/2006-04/2006	Co-op Research Student. Bacteriophage and toxin quantification research. Gangagen Life Sciences, Inc., Ottawa.
05/2005-08/2005	Co-op Research Student. Mycological isolation and identification studies. Agricultural and Agri-Food Canada, Ottawa.
09/2004-12/2004	Co-op Research Student. High throughput preparation of SAGE libraries for stem cell research using robotic equipment. Ontario Genomics Innovation Centre, Ottawa.

Awards and Honours

09/2008-present	Ontario Graduate Scholarship
09/2008-present	University of Ottawa Excellence Scholarship

09/2007-08/2008	CIHR Canada Graduate Scholarship Master's Award
09/2007-08/2008	University of Ottawa Excellence Scholarship
06/2007	Graduated *magna cum laude*, B.Sc. Biochemistry with Co-operative Education
2006	CAFCE Co-op Student of the Year Nomination
2005	Roger Guindon Scholarship.
2005	Constance Nozzolillo Scholarship
09/2004-12/2005	University of Ottawa Merit Scholarship
09/2003-04/2007	Dean's Honour List
09/2002-04/2003	University of Ottawa Admission Scholarship

Graduate Classes Completed

BCH8109 – Advanced Topics in Cell Death (A^+)

BCH8103 – Advanced Topics in Gene Expression and Protein Synthesis (A^+)

Abstracts

"The Regulation of the X-Linked Inhibitor of Apoptosis Protein (XIAP) through Alternative Non-Coding Regions." Ontario Institute for Cancer Research's 2nd Annual Scientific Meeting. February 22-24, 2009. Alliston, Ontario.

Presentations

01/2009 Invited speaker. The bi-weekly RNA Club lecture series. "Regulation of XIAP expression by distinct 5' untranslated regions".